**NKFI K125477 Final report**

# Antiinflammatory therapies for enhancing tissue regeneration

**Péter Gogolák**
**University of Debrecen, Institute of immunology**

Neutrophil granulocytes play an important role in tissue inflammation. Their presence influences the course of the tissue inflammatory process induced by infections or injuries. This process has an influence on tissue regeneration, both directly and indirectly

## Investigations of tissue regeneration and inflammation in neutrophil deficient mice

In our project, we investigated a neutrophil granulocyte deficient mouse model. The model uses a myeloid cell specific knock out of the Mcl1 anti-apoptotic gene with the help of the Cre-Lox recombination system, driven by the expression of the Lyz2 (lysozyme 2) gene promoter. The Mcl1 gene is the most important anti-apoptotic gene in neutrophil granulocytes. Its myeloid lineage specific defect results in severe neutropenia in mice, but there were no recognized other deficiency described until recently (1, 2).

We used a well-known tissue injury model, and we observed alterations in muscle regeneration after cardiotoxin induced muscle injury in control (wild type, WT) and neutrophil deficient mice. We observed significant cellular differences in the injured muscles of the control and neutrophil deficient mice. As expected, we could hardly find neutrophil granulocytes in the tissues of neutrophil deficient mice one day after muscle injury. The number of immigrating monocyte-derived macrophages was also lower. The number of $F4/80^{+}$ macrophages was also lower a few days after the tissue injury. 8 days post injury, we could not find differences in the structure of the regenerating muscle fibers by histology, but in the case of the neutrophil deficient mice, we observed an elevated presence of adipose tissue cells, and mononuclear leukocytes. We developed a simplified flow cytometric method to evaluate the number of the most important muscle precursor cells. We did not observe significant differences in the number of satellite cells ($Lin^{-}$, $Sca1^{-}$, $\alpha7\text{-integrin}^{+}$), and fibro-adipogenic progenitor cells ($Lin^{-}$, $Sca1^{++}$, $CD140a^{+}$) between the injured muscles of the control and neutrophil deficient mice. This method was briefly described in the following articles:

*Zsófia Budai et al. Impaired Skeletal Muscle Development and Regeneration in Transglutaminase 2 Knockout Mice, Cells . 2021 Nov 9;10(11):3089. doi: 10.3390/cells10113089., 2021.*

*Nastaran Tarban et al. Regenerating Skeletal Muscle Compensates for the Impaired Macrophage Functions Leading to Normal Muscle Repair in Retinol Saturase Null Mice, Cells 2022, 11(8), 1333, 2022*

We plan to publish an article describing this methodology in detail in the Cytometry journal.

We showed that the increased leukocyte number in the neutrophil deficient mice can be attributed to the presence of T cells. A significantly higher number of conventional (αβ) and gamma-delta (γδ) T cells can be found in the muscle post injury. As previous examinations by different workgroups could not find differences in the cellular composition of the blood, bone marrow and spleen of the animals (1, 2), we performed several investigations to find an explanation for the differences in T cell numbers. We showed alterations in the bone marrow of the control and neutrophil deficient animals. The bone marrow of the neutrophil deficient animals contains fewer erythrocytes even observed by naked eye. There are huge number of atypical neutrophil granulocyte in it, which cannot be found in the

circulation of the animals. The spleen of the neutrophil deficient animals became larger by the age compared to the control. We detected higher number of common myeloid precursor cells in it, which could give rise both granulocyte and erythrocyte precursor cells.

Several other findings of our investigations were summarized in the article we sent to the FEBS Letters. The proof of this article is attached to the end of this document. Unfortunately, referee asked major revisions and proposed reworking of the article.

Recently we prepared additional histology data to prove our hypothesis about the extramedullary granulopoiesis and erythropoiesis within the spleen (Figure 1). We measured additional inflammatory markers in the circulation of the neutrophil deficient animals. In addition of the previously shown serum amyloid P (SAP) concentration difference, the CXCL2 (IL-8-like chemokine in mice) concentration is also increased in neutrophil deficient mice. We want to show with our data that the elevated T cell number is a general consequence of the inflammation in the neutrophil deficient mice, therefore we conducted a classic experiment in which we induced peritonitis in mice injecting a thioglycolate medium into the peritonea. We measured significantly elevated number of T cells in neutrophil deficient mice compared to the control. After these experiments, we will resubmit our reworked article to the editors.

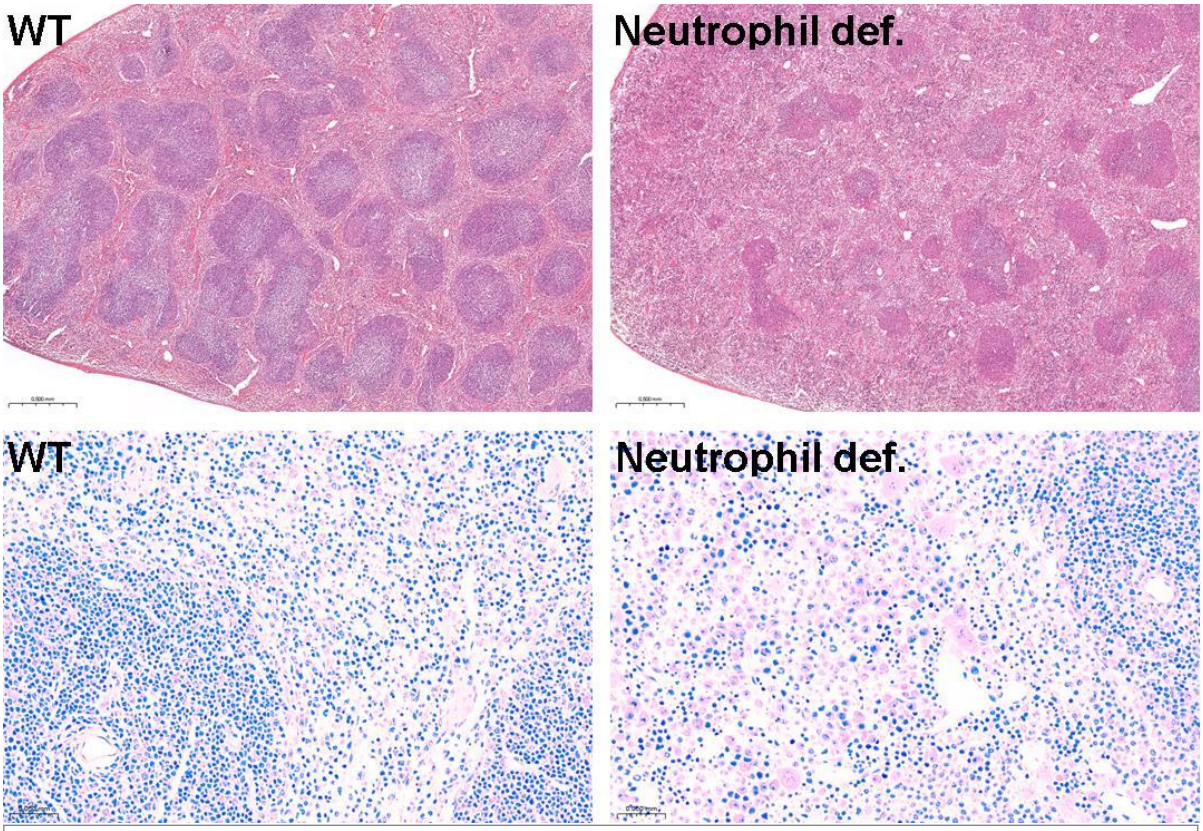


***Figure 1.*** *Comparative histology of the spleen in control (WT) and neutrophil deficient mice. Upper panels, hematoxylin-eosin staining: The spleen of the neutrophil deficient animals shows irregular red pulp and white pulp organization. The area, representing the red pulp is more pronounced. The lymphocyte rich white pulp areas are smaller and scattered. Lower panels, May-Grünwald-Giemsa staining: The red pulp of the neutrophil deficient mice spleen contains many large irregular cells. Their cytoplasms are thick, their nuclei have euchromatic staining. They may represent dividing, developing myeloid progenitor cells.*

## Investigation of T cell functions in neutrophil granulocyte deficient mice

The elevated T cell number in inflammation of the neutrophil granulocyte deficient mice can influence the immunization of the animals. Adjuvants (CFA or alum) injected in the peritoneal cavity of neutrophil deficient mice result in an elevated number of immigrating T cells within the peritoneal cavity compared to the wild type control (Figure 2).

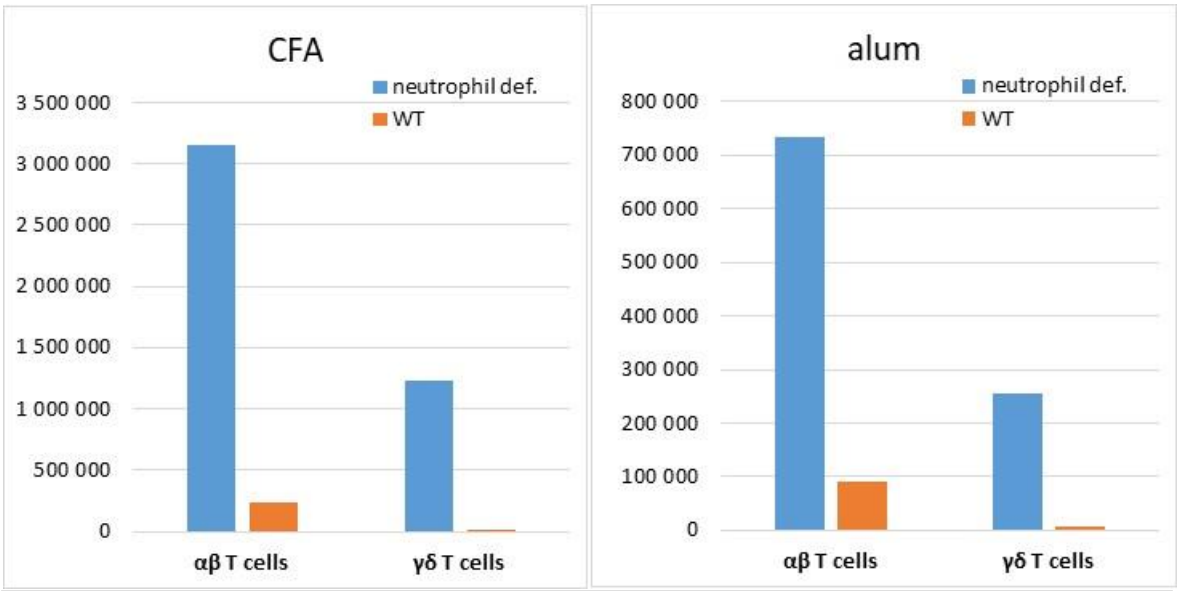


***Figure 2**. T cells in the peritoneal lavage of control (WT) and neutrophil deficient mice. Mice peritonea were injected with complete Freund adjuvant (CFA) or alum adjuvant. Peritonea were washed 3 days after the treatment, and the T cell numbers were evaluated by flow cytometry.*

We immunized mice with bovine serum albumin (BSA) as an antigen in the presence of Freund adjuvant or alum adjuvant. We observed a slight increase in antigen-specific primary IgM production both in the presence of complete Freund adjuvant (CFA) and alum adjuvant. The difference can be observed after the second immunization in the case of Freund adjuvant, but there was no difference in the case of alum adjuvant (Figure 3). T cell-dependent IgG1 antibodies can rapidly appear after the first immunization in the circulation of mice deficient in neutrophils only. The differences between the control and neutrophil deficient mice disappeared after the second immunization (Figure 4). The immunomodulatory mechanism of the alum adjuvant is not clear even after almost a century of usage. Some theories suggest the NETosis-inducing effect of the alum on neutrophils as an explanation of the booster effect (3). Our immunization experiments weaken this hypothesis, as in the presence of alum adjuvant, the antigen-specific antibody response of neutrophil deficient mice was superior compared to the control. We would like to submit our results concerning these immunization experiments to the MDPI Antibodies journal.

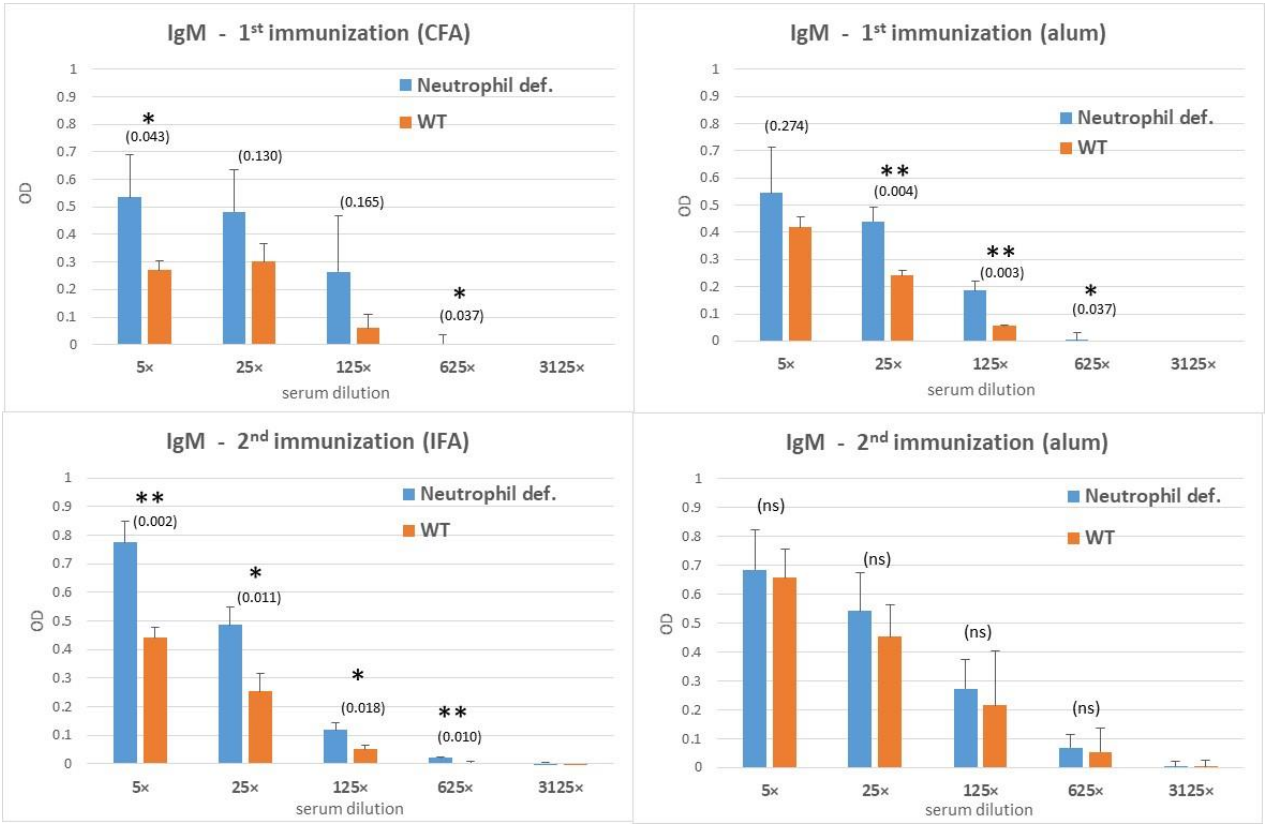


***Figure 3***. *ELISA of antigen (bovine serum albumin, BSA) specific serially diluted mice sera. Upper panels: The amount of BSA specific IgM is higher in neutrophil-deficient mice after the primary immunization with both in the case of CFA (left panel) and alum adjuvant (right panel). Lower panels: The difference is evident after the second immunization with IFA adjuvant (bottom left panel). There is no significant difference between the amounts of antigen specific serum IgM after the 2nd immunization with alum adjuvant (bottom right panel). Significances are indicated with asterisks. The probability values of the significances are indicated in parentheses. ns – not*

## Mice deficient in neutrophil granulocytes as a tool to investigate T cell functions in different inflammatory conditions

The increased number of immigrating T cells in the inflamed tissues of neutrophil granulocyte deficient mice provide opportunities to investigate these cell populations. In control animals, the available T cell number is rather low for the additional investigations, e.g., for transcriptomics. The rare cell populations, e.g., some of the γδ T cell numbers are exceptionally low, so their investigations are very difficult. As part of the project closure, we continuously collect the mRNA of isolated αβ- and γδ T cells from inflamed muscle tissue for later transcriptomic purposes.

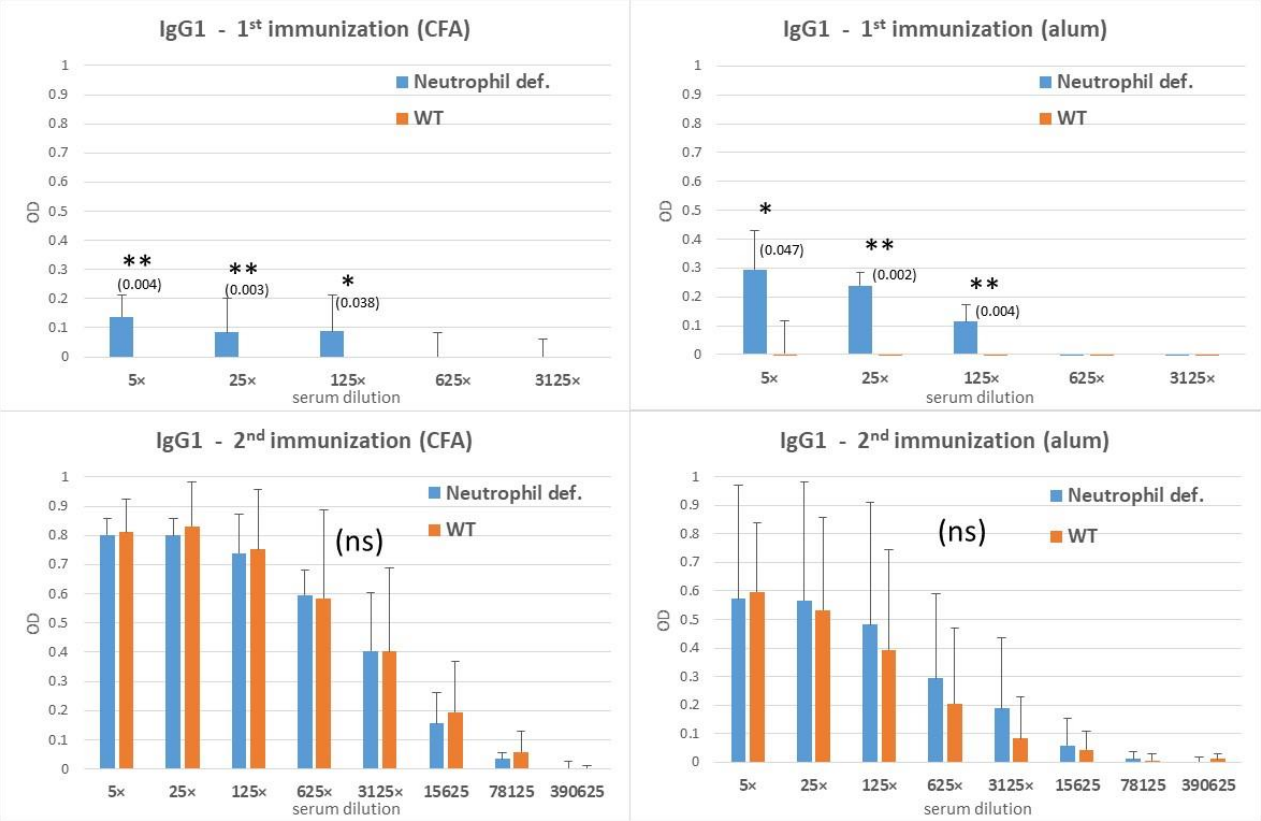


***Figure 4****. ELISA of antigen (bovine serum albumin, BSA) specific serially diluted mice sera. Upper panels: BSA specific IgG1 appeared after the first immunization of neutrophil deficient mice both with the use of Freund adjuvant (left panel) or alum adjuvant (right panel). There was no detectable IgG1 production in the control (WT) mice one week after immunization. Lower panels: There was no difference in the amount of BSA specific serum IgG1 after the 2nd immunization. Significances are indicated with asterisks. The probability values of the significances are indicated in parentheses. ns – not significant*

## Justification of major deviations from the budget

The budget amount described in section 1.2.2, for the processing of muscle tissue samples, was not realized due to the circumstances of the COVID-19 pandemic. We used the budget for the procurement of supplies during the extension of the grant period.

The budget for the costs of participating in foreign conferences described in section 3.1 was not used due to the circumstances of the COVID-19 pandemic. We used this budget also for the procurement of supplies during the extension of the grant period.

We used the budget amount of section 4 (instead of a Unix-based computer) to replace the malfunctioning water purification equipment of the Immunology Institute. The ion exchanger - filter - water purifier is indispensable for the production of buffers and reagents necessary for experimental work.

**References:**


1. *Dzhagalov, I. et al. The antiapoptotic protein Mcl-1 is essential for the survival of neutrophils but not macrophages. Blood, 2007. 109(4): p. 1620-6.*
2. *Csepregi, J.Z., et al. Myeloid-Specific Deletion of Mcl-1 Yields Severely Neutropenic Mice That Survive and Breed in Homozygous Form. J Immunol, 2018. 201(12): p. 3793-3803.*)
3. *Stephen J. et al. Neutrophil swarming and extracellular trap formation play a significant role in Alum adjuvant activity. Npj Vaccines. 2017; 2(1): 1-8.*

FEBS Letters

FEBS PR
science publishing b

# Elevated T cell number in muscle injury may compensate for the effects of missing neutrophil granulocytes in neutrophil-deficient mice

| | |
|---|---|
| Journal: | *FEBS Letters* |
| Manuscript ID | Draft |
| Wiley - Manuscript type: | Research Article |
| Date Submitted by the Author: | n/a |
| Complete List of Authors: | Halász, Hajnalka; University of Debrecen, Doctoral School of Molecular Cell and Immune Biology, Faculty of Medicine<br>Dezső, Balázs; University of Debrecen, Institute of Pathology, Faculty of Medicine; University of Debrecen, Department of Oral Pathology and Microbiology, Faculty of Dentistry<br>Pap, Attila; University of Debrecen, Department of Biochemistry and Molecular Biology, Faculty of Medicine<br>Mócsai, Attila; Semmelweis University, Department of Physiology, Faculty of Medicine<br>Nagy, Laszlo ; University of Debrecen, Department of Biochemistry and Molecular Biology, Faculty of Medicine<br>Varga, Tamás; Debreceni Egyetem, Department of Biochemistry and Molecular Biology, Faculty of Medicine<br>Gogolák, Péter; University of Debrecen, Department of Immunology, Faculty of Medicine |
| Keywords: | muscle regeneration, neutrophil deficiency, increased gamma-delta T cell number, γδ T cells, increased T cell number, eosinophils, extramedullary haematopoiesis, splenomegaly, extramedullary leukopoiesis |
| Abstract: | In our study, we used a genetically modified mouse model deficient in neutrophil granulocytes to investigate the consequences of their absence on muscle tissue regeneration. Our observations revealed changes in muscle regeneration and several previously unrecognized cellular and tissue discrepancies in the animals. As a direct or indirect effect of neutrophil deficiency, we found a decreased number of macrophages in inflamed tissue and a surprisingly high number of αβ- and γδ T cells. Alterations in the cellular compartment of the bone marrow resulted in paler bone color and erythroid cell-specific bone marrow insufficiency, which was compensated for by extramedullary hematopoiesis and splenomegaly. |
| | |

# Elevated T cell number in muscle injury may compensate for the effects of missing neutrophil granulocytes in neutrophil-deficient mice

Hajnalka Halász[1, 2], Balázs Dezső[3,4], Attila Pap[5], Attila Mócsai[6], László Nagy [5#], Tamás Varga[5#] and Péter Gogolák[2#*]

1 Doctoral School of Molecular Cell and Immune Biology, Faculty of Medicine, University of Debrecen, Hungary; halaszhajni0329@gmail.com (H.H.)
2 Department of Immunology, Faculty of Medicine, University of Debrecen, Debrecen, Hungary; gogy@med.unideb.hu (P.G.)
3 Department of Oral Pathology and Microbiology, Faculty of Dentistry, University of Debrecen, Debrecen, Hungary
4 Institute of Pathology, Faculty of Medicine, University of Debrecen, 4032 Debrecen, Hungary; bdezso@med.unideb.hu (B.D.)
5 Department of Biochemistry and Molecular Biology, Faculty of Medicine, University of Debrecen, 4032 Debrecen, Hungary; papattila1001@gmail.com (A.P.); tamasvarga9223@gmail.com (T.V.); nagyl@med.unideb.hu (L.N.)
6 Department of Physiology, Faculty of Medicine, Semmelweis University, Budapest, Hungary; mocsai.attila@med.semmelweis-univ.hu (A.M.)

* Correspondence: University of Debrecen, Faculty of Medicine, Department of Immunology, 1. Egyetem Square, Debrecen, H-4032, Hungary. Tel/Fax: +36 52 417 159, e-mail: gogy@med.unideb.hu
# These authors share last authorship



## Abstract:

In our study, we used a genetically modified mouse model deficient in neutrophil granulocytes to investigate the consequences of their absence on muscle tissue regeneration. Our observations revealed changes in muscle regeneration and several previously unrecognized cellular and tissue discrepancies in the animals. As a direct or indirect effect of neutrophil deficiency, we found a decreased number of macrophages in inflamed tissue and a surprisingly high number of αβ- and γδ T cells. Alterations in the cellular compartment of the bone marrow resulted in paler bone color and erythroid cell-specific bone marrow insufficiency, which was compensated for by extramedullary hematopoiesis and splenomegaly.

**Keywords:** muscle regeneration; neutrophil deficiency; increased gamma-delta T cell number; γδ T cells; increased T cell number; eosinophils; extramedullary haematopoiesis; splenomegaly

**Abbreviations:** CTX – cardiotoxin 1; DAMP – damage-associated molecular pattern; Mcl1 – the gene of the "Induced myeloid leukemia cell differentiation" anti-apoptotic protein; Mcl1ΔMyelo – The myeloid cell type deficient inactivation of the Mcl1 gene ($Lyz2^{Cre/Cre}Mcl1^{flox/flox}$ genotype); p.i. – post injury; RCF – relative centrifugal force (g); RPM – revolution/minute; SAP – serum amyloid P component (pentraxin 2, acute phase protein); TA – tibialis anterior (in the context of injured muscle); WT – wild type (genotype);

## Introduction

In our study, we aimed to reveal the effect of neutrophil granulocyte deficiency on muscle tissue regeneration. Our investigations shed light on several changes in the cellular events of tissue injury

and the subsequent regeneration process in neutrophil grenulocyte deficient mice. We even described organ-level changes that are mediated directly or indirectly by the absence of neutrophil granulocytes.

Genetically modified mice are commonly used for research or as animal models of human diseases. Conditional gene knockout models are techniques that can be applied to eliminate the effect of a specific gene from a certain tissue or cell type. With the help of conditional gene knockout models, it is possible to eliminate specific gene-dependent cell types without detrimental effects on embryonic development. The most commonly used technique is the Cre-lox recombination system [1].

The Cre-loxP recombination system can be used to induce the selective depletion of Mcl1 anti-apoptotic gene. Neutrophils express several pro-apoptotic members of the Bcl-2 family (such as Bax, Bad, Bak, Bid and Bik), and only a few ant apoptotic proteins, such as Mcl-1 and A1 [2]. Mcl1 is essential for the survival of neutrophil granulocytes [2]. The Lyz2 (alias LysM) gene promoter-driven expression of the Cre recombinase excises the loxP sequence-flanked (floxed) gene regions of the Mcl1 gene in cells that have active lysozyme 2 expression. This process severely affects developing neutrophil granulocyte precursors after they start synthesizing and storing lysozyme [2]. It induces severe neutropenia in homozygous $Lyz2^{Cre/Cre}Mcl1^{flox/flox}$ mice without directly affecting other immune cells and with mostly normal survival and fertility under conventional conditions [2, 3]. Such mice are refered to in the literature as Mcl-$1^{-/-}$ or Mcl1ΔMyelo genotype mice [2, 3]. We use the latter term in this article to refer them (see also the Materials and Methods).

Due to their major role in eliminating invading microorganisms, neutrophil granulocytes were considered simple „dumb" suicide killers for a long time. In recent decades, this view of neutrophils has begun to change [4]. Through cell-cell interactions or by secreting cytokines, chemokines or other factors, neutrophils can modulate the activation of several cell types [5-8]. These cell types (e.g., macrophages) can play a crucial role in tissue remodeling and repair. Neutrophils can even have immunomodulatory effects on T- and B-lymphocytes [9, 10].

Tissue injuries and regeneration are strongly influenced by the inflammatory and the subsequent resolving process influenced by the immune system [11, 12]. Muscle injury can be rapidly resolved due to its remarkable regenerative capacity [13]. One of the most widely used muscle injury models involves injecting Cobra (Naja sp.) venom component cardiotoxin 1 (CTX) into the tibialis anterior (TA) muscle of mice [14]. Intramuscular injection of CTX induces acute muscle fiber necrosis, resulting in rapid recruitment of inflammatory cells and culminating in inflammation.

Neutrophils are the first cell type to arrive in inflamed tissue from the circulation. In cases of injury or infection, they can be attracted directly by chemotactic materials (DAMPs, alarmins) released from necrotic tissues [15-17]. Tissue sentinel cells (e.g., tissue-resident macrophages, mast cells, innate lymphoid cells) can also be activated by these materials and subsequently produce neutrophil-attracting chemokines [18]. In inflamed tissue, neutrophils secrete chemokines and pro-inflammatory cytokines to recruit blood-derived monocytes [19]. Immigrating monocytes differentiate into $Ly6C^{++}$ inflammatory monocytoid macrophages in injured necrotic tissue. These inflammatory cells produce inflammatory cytokines (e.g., TNF) that activate muscle stem cells (satellite cells, SATs) [20] in the injured muscle to proliferate and become myoblasts [21, 22].

Neutrophil granulocytes can have both regeneration-prone and regeneration-delaying effects in tissue injuries [23, 24]. They can begin to clear away necrotic tissue debris. In large numbers, they can confer high arginase activity, which can even modulate T-cell function [25]. Later, they die by apoptosis. The decreased amount of necrotic debris and the large number of apoptotic neutrophils induce switch in the differentiation program of the $Ly6C^{++}$ inflammatory macrophages during the

efferocytosis process. The appearing re-programmed F4/80$^{+}$ Ly6C$^{low}$ macrophages have resolving functions [26, 27]. They can support the reparative phase of myogenesis following the initial proliferative phase by producing anti-inflammatory cytokines [28], influencing other tissue precursor cells – such as fibro-adipogenic precursor (FAP) cells - or secreting other bioactive materials that induce the formation of myofibers from myoblasts or mediating tissue revascularization [29]. Neutrophil granulocytes influence these processes either directly or indirectly.

Our observations support the regeneration-prone effect of neutrophil granulocytes in CTX-induced muscle injury. We investigated these events in Mcl1ΔMyelo mice mainly at the cellular level. Our results emphasize that the proper interpretation of experimental findings strongly depends on appropriate knowledge about experimental models.

## Materials and Methods

### Mice

The animal experiments were performed in accordance with Hungarian and European regulations approved by the Animal Care and Use Committee of the University of Debrecen (DEMÁB) with permission number 16/2019/DEMÁB.

2-4 months old Lyz2$^{Cre/Cre}$ Mcl1$^{flox/flox}$ (*Lyz2*$^{tm1(cre)Ifo/tm1(cre)Ifo}$*Mcl1*$^{tm1Ywh/tm1Ywh}$; referred to as Mcl1ΔMyelo) mice on the C57BL/6 genetic background [3] were used in the experiments which were bred under specific pathogen-free conditions. These mice can be bred in homozygous and heterozygous form too, so their genotypes should be determined by allele-specific PCR.

### Genotyping

Total DNA was extracted from tissue samples gained by tail biopsy or toe clipping [30]. The tissues were digested by 1 hour incubation on 98°C in 25 mM NaOH, 0.2 mM EDTA solution. The digested samples were neutralised and centrifuged in 41 mM TRIS-HCl for 5 minutes, in micro centrifuge with 1500 RCF (or ~4000 RPM in micro centrifuge with 85mm rotor). The supernatants contained the extracted DNA after centrifugation. The samples can be stored on 4°C or on -20°C for a longer period.

PCR primers were ordered from Integrated DNA Technologies Inc., Coralville, Iowa, USA (https://eu.idtdna.com/ - last checked in January 2023). PCR master mix was prepared from: nuclease free water (R0581, Thermo-Fisher Scientific, Waltham, MA, USA), 10x Taq buffer with KCl (B38, Thermo-Fisher Scientific, Waltham, MA, USA), 20 µM Forward primer (Mcl1 flox fw. sequence 5' GGT TCC CTG TCT CCT TAC TTA CTG TAG 3'), 20 µM Reverse primer (Mcl1 flox rev. sequence 5' CTC CTA ACC ACT GTT CCT GAC ATC C 3'), 25 mM $MgCl_2$ (R0971, Thermo-Fisher Scientific, Waltham, MA, USA), 2,5 mM dNTP (R0181, Thermo-Fisher Scientific, Waltham, MA, USA), 5 U/µl Taq polymerase (EP0402, Thermo-Fisher Scientific, Waltham, MA, USA) and extracted DNA. PCR protocol: 95°C – 2 minutes; 35 cycles of: 94°C – 1 minute, 60°C – 1 minute, 72°C – 1 minute; 72°C – 5 minutes; samples can be stored on 4°C. The fragments of DNA were separated by electrophoresis in a 1.5% agarose gel supplemented with Ethidium bromide. A band at 250 base pairs (bp) denotes Mcl1 WT mouse, a band at 357 bp denotes Mcl1ΔMyelo mouse, bands at both sites (250 and 357 bp) are for Mcl1 flox/+ heterozygous mouse (Supplementary figure S1). The PCR reactions were performed by Hybaid PCR Express Thermal Cycler machine (Thermo Electron Corporation / Thermo Fisher Scientific). The gels were documented by Azure C300 Gel Imager (Azure Biosystems, Dublin, CA, US).

### Cardiotoxin-induced sterile inflammation and the processing of the tissues

Sterile muscle inflammation was induced by injection of 50 µl of $12\times10^{-6}$ M cardiotoxin 1 (CTX) (L8102-1MG, Latoxan, Portes-lès-Valence, France) into the tibialis anterior muscles. Inflamed tissues were isolated and processed at different times after injection based on protocol of Guardiola O. et al [31]. The muscles were either used for histology or the cells were obtained by digestion of muscles with collagenase B (C6885-1G, Sigma Aldrich, St. Louis, USA) and the suspension is purified by filtration through an 100 µm, then a 40 µm cell strainers (43-50040-51 and 43-50100-51, PluriSelect, Leipzig, Germany). The cell suspensions were analysed by flow cytometry.

**Histology**

Day 8 post injury muscles were removed and snap frozen in nitrogen-chilled isopentane and kept at −80 °C until analysis. The frozen tissue samples were oriented and 8 µm thick cryosections were cut, perpendicular to the muscle fibers, and stained with haematoxylin-eosin (HE) with standard methods. The tissue sections of the samples represent at least 70% of the CTX-injured muscle region. The HE-stained serial tissue sections were digitalized using Pannoramic MIDI digital slide-scanner (3D-Histech Co., Budapest, Hungary) utilizing Zeiss Plan-Apochromat objective (magnification: 20x/0.8 NA) and Hitachi (HV-F22CL) 3CCD progressive scan colour camera. Image analysis for each group was performed by the HistoQuant application of Pannoramic Mirax Viewer software 1.15.2. (3D-Histech). If applicable, at least four (ranging from 2 to 6) necrotic or inflammatory cellular foci were selected randomly in each specimen per group for analytic measurements. The photo documentations on representative regions were carried out from the scanned slides using the Mirax-Viewer software.

**Flow cytometry analysis**

Cell suspensions, obtained from different tissues, were prepared for flow cytometry analysis. The samples were divided into small aliquots according to the numbers of stainings. The samples were pre-incubated with TruStain FcX PLUS anti-mouse CD16/32 (156604, BioLegend, San Diego, USA) and with heat inactivated normal rat serum (10710C, Invitrogen, Carlsbad, USA) for blocking. For calculating the absolute cell counts, a known number of polystyrene micro particles, size 8 µm (78511, Sigma Aldrich, St. Louis, MO, USA) were added to each freshly prepared sample stock. Cells were washed with “FACS buffer” (PBS – pH=7,2 – supplemented with 0.5% BSA, 0.05% sodium azide and 2mM EDTA) and centrifuged down, with 500g relative centrifugal force, then incubated with the prepared antibody cocktails for 30 minutes on ice in the dark. After the incubation, the cells were washed again. Measurements were performed using ACEA NovoCyte 2000R or BD FACSAria III flow cytometers. Data were analysed with the help of FlowJo Software (Tree Star / Becton Dickinson, New Jersey, NJ, USA).

The following antibodies were used for labelling. Several reagent were purchased from BioLegend (San Diego, CA, USA): FITC or BV785 anti-mouse CD45 (clone 30-F11, cat. 103108 and 103149 respectively), FITC or PerCP/Cyanine5.5 anti-mouse/human CD11b (Mac-1) (clone M1/70, cat. 101206 and 101228 respectively), APC anti-mouse F4/80 (clone BM8, cat. 123115), APC anti-mouse Ly6G (clone 1A8, cat. 127614), PerCP/Cyanine5.5 and APC/Fire750 anti-mouse Ly6C (clone HK1.4, cat. 128012 and 128045 respectively), PerCP/Cy5.5 anti-mouse CD45 (clone I3/2.3, cat. 147705), PE anti-mouse CD19 (clone 6D5, cat. 115507), APC anti-mouse CD3ε (clone KT3.1.1, cat. 155605), FITC anti-mouse CD90.2 (clone 30-H12, cat. 105305), FITC anti-mouse TCR β chain (clone H57-597, cat. 109205), PE anti-mouse TCR γ/δ (clone GL3, cat. 118107), PE anti-mouse CD117 (c-Kit) (clone ACK2, cat. 135105), biotin anti-mouse TER-119/Erythroid Cells (clone TER-119, cat. 79748), biotin anti-mouse Ly6G/Ly-6C (Gr-1) (clone RB6-8C5, cat. 79750), biotin anti-mouse/human CD45R/B220 (clone

RA3-6B2, cat. 79752), biotin anti-mouse CD11b (clone M1/70, cat. 79749), biotin anti-mouse CD3ε (clone 145-2C11, cat. 79751), FITC Streptavidin (cat. 405201), APC Streptavidin (cat. 405207).

Antibodies purchased from BD Biosciences (New Jersey, NJ, USA): BV605 Rat anti-mouse Ly-6A/E (Sca1) (clone D7, cat. 563288), BV711 Rat anti-mouse CD127 (clone SB/199, cat. 565490)

We had several "issues" with the CD34 monoclonal antibodies. Finally, the BV421 anti-mouse CD34 (clone: SA376A4, rat IgG2a) from Sony Biotechnology was the ideal source. BV711 conjugated Ly6G (clone 1A8, cat.1238215), BV711 conjugated TCR β chain (clone H57-597, cat. 1146215) antibodies were also obtained from Sony Biotechnology.

Anti-SiglecF APC, mouse (130-102-241, Miltenyi Biotec, Bergisch Gladbach, Germany), Anti-CD125 (anti-IL-5 receptor alpha chain, 130-106-031, Miltenyi Biotec, Bergisch Gladbach, Germany) and SYTO16 green fluorescent cell permeant nucleic acid stain (S7578, Invitrogen, Carlsbad, CA, USA) were also applied for staining. Cell non-permeant "viability" dyes were obtained from Thermo-Fisher Scientific, Waltham, MA, USA: SytoxAAD (cat. S10349), 7-AAD (cat. A1310).

**Determination and interpretation of the absolute cell count within the examined samples**

Absolute cell number were determined from the flow cytometric measurements by the help of polystyrene microparticles ("counting beads") (8 µm, Sigma Aldrich, St. Louis, MO, USA, cat.nr. 78511) with characteristic high side directional light scattering (SSC) and homogenous small forward light scattering (FSC) (Supplementary figure S2). The number of the beads were pre-determined with microscopic particle counting in Bürker-chamber. Known number of "counting beads" were applied in the sample stocks. The measured cell number was compared with the measured bead number, and the original absolute cell number from the starting sample were calculated back according to their ratio. Usually $4.5\times10^5$ beads were added to the left and right freshly prepared TA muscle cell suspension of the animals. The freshly prepared bone marrow cell suspension from the left and right femoral bones and the freshly prepared spleen cell suspension were supplemented with the same number of counting beads. Blood leukocyte absolute numbers were determined from 100µl blood of the animals similarly, after the lysis of the erythrocytes. The only exception was the mature erythrocyte number determination within the blood samples, where $1\times10^6$ beads were added to 10µl blood sample to get high enough bead counts to calculate back effectively the erythrocyte numbers.

**Blood, bone, spleen and lymphoid tissue processing for the characterization of the cells**

Preparation of cell suspensions from bone marrow, spleen and blood was performed by routine protocols of other researchers with some modifications [32, 33]. Bone marrow cells were obtained from femur and tibia by flushing with sterile, ice-cold PBS buffer.

Rapid bone marrow isolation involved small (200µl) capped tubes, which were punctured by a fine syringe needle on the bottom. The femoral bones' epiphyses were superficially cut at both end to open them and the prepared bones were placed inside the punctured tubes. The punctured tubes – with the bones – were placed inside a larger (1.5ml) snap cap tube, and spun down in a micro centrifuge with a rapid (~10 sec) speed increase to reach the maximum spin (~13000 RPM, ~16000 RCF) then left to slow down. The bone marrow was collected from the bottom of the 1.5ml snap cap tubes.

Immune cells from the spleen were gained by crushing the tissue with a sterile syringe piston in petri dishes. Cell suspensions were filtered through 100 µm cell strainers to purify the samples from large tissue debris, then washed and centrifuged.

Blood samples were collected from orbital sinus or by cardiac puncture [34]. The cellular elements were determined and characterized by flow cytometry.

Macro photographs of the mouse spleens and bones were taken with a Redmi Note 6 smartphone. Image brightness and contrast were adjusted to increase the visible difference between existing shades of the samples using GIMP 2.10 image processing software (https://gimp.org/ - last checked in January 2023).

**Quantitative determination of Mouse Petraxin 2/SAP concentration with Quantikine ELISA**

Blood samples were collected from mice of different ages and sera were obtained by centrifugation. Samples were stored at -20°C. Concentration of Serum Amyloid P Component (SAP) was determined by Mouse Pentraxin 2/SAP Immunoassay kit (MPTX20, R&D Systems, Minneapolis, MN, USA). The assay procedure was performed according to the manufacturer's recommendations. The samples were diluted 1:200, the optical density was measured at 450 nm with Synergy HT Elisa Reader. The results were evaluated with Microsoft Office Excel software.

**Data and statistical analysis**

Data analysis was performed using Microsoft Excel and SigmaStat software. Student's t-test was used in the comparison of data sets, unless a different test was suggested by the SigmaStat software (Mann-Whitney U test, when the data distribution normality test had failed). GraphPad Prism 6 software was used for the representation of results. On the figures, the error bars represent standard deviations (SD). The p values of $<0.05$ were considered statistically significant.

## Results

**Microscopic histopathology**

Apart from some comparable morphological similarities in the reparative cellular processes of skeletal muscle tissue, obvious differences can also be identified in the regeneration of CTX-damaged muscle when comparing WT with Mcl1ΔMyelo mice. Regarding the similarities, the lesional tissues from both groups develop newly formed immature muscle fibers by day 8 post-injury (p.i.), most likely from perimyseal myogenic stem cells that differentiated into myocytes which in turn organized into muscle fibers composed of centrally located or multinucleated myocytes (Figure 1).

Nevertheless, remarkable differences in the dynamics and pattern of muscle renewal between WT and neutrophil-deficient (Mcl1ΔMyelo) mice can also be recognized. Accordingly, CTX-induced muscle damage in WT (control) mice shows a morphologically coordinated regeneration at this time, resulting in well-organized and rather uniform muscle fiber formations and decreased perimyseal cellular activities with the presence of few macrophage-type mononuclear cells along protein-rich edematous (yet non-fibrotic) septa (Figure 1 A, dark blue arrows).

In contrast, following CTX-induced muscle injury in Mcl1ΔMyelo mice, the regenerative response appears delayed in cleaning the tissue from dead or damaged parenchymal and accessory cells, resulting in traces of necrotic tissue residues in the lesion even at day 8 p.i. (Figure 1 B1 insert). This is probably one reason for the increased number of intramuscular adipocytes arising from fibro-adipogenic progenitor (FAP) accessory cells (Figure 1 B, vacuolar cells, light blue arrows), to substitute for missing parenchymal myogenic cells (the process is also called lipomatous atrophy), highlighting incomplete muscle restoration at this time. This is confirmed by the fact that in well-regenerating CTX-damaged skeletal muscle of WT mice there is a lower number of intramuscular adipocytes by day 8 p.i. (Figure 1 A1 vs. B1, light blue arrows).

The protracted regeneration in Mcl1ΔMyelo mice is strictly associated with changes in the qualities and quantities of intramuscular inflammatory cells recruited to the lesion in response to muscle injury. As shown in Figure 1 B, the predominant cell type are lymphocyte-like mononuclear cells characterized by small round darkly stained nuclei with inconspicuous cytoplasms (a few indicated with green arrows), and several cells that have undergone single cell necrosis where no nuclear staining is seen (a few indicated by green arrowheads).

**Leukocytes in the injured muscle tissue**

The healthy tibialis anterior muscle of the mice contains only a few thousand $CD45^+$ leukocytes. Approximately half of them are $CD11b^+$ (also known as Mac-1) of myeloid origin – probably resident macrophages – and the other half are small CD11b negative lymphocyte-like cells – probably innate lymphoid cells (data not shown).

We examined the leukocyte numbers within the injured TA muscles in different time points after the CTX injection and compared the differences between the wild type and the Mcl1ΔMyelo mice. We had prepared the TA muscles of the injured mice and processed them to cell suspensions. The cellular composition of the samples was evaluated by flow cytometry after staining the cells with different cell line specific, fluorescence labelled monoclonal antibodies (Figure 2 B, D). As the Gr-1 antibody (clone RB6-8C5) recognises Ly6G and cross-reacts with the Ly6C molecules [35-37], we used a direct Ly6G specific monoclonal antibody (clone 1A8) to detect neutrophil granulocytes. Representative pictures of the cytometric measurements and the gating strategies can be seen in the Supplementary picture set (Supplementary figure S3). Obviously, there were large differences in the immigrating $CD11b^+$ $Ly6G^+$ neutrophil granulocyte numbers one day after the initiation of the muscle injury and at day 2 post injury.

The neutrophil granulocyte number sharply fell in the injured muscle at day 3, which could be attributed to the neutrophils' continuous apoptosis and their subsequent efferocytosis within the tissue of the wild type mice (Figure 2 B, C). The almost complete absence of neutrophils could be a cause of the lower leukocyte number in the tissue of Mcl1ΔMyelo mice a day after injury, as seen in the comparison of $CD45^+$ leukocyte number with the WT mice (Figure 2 A). We found large differences in the number of the $Ly6C^{++}$ immigrating monocytoid macrophages. The Mcl1ΔMyelo mice have lower number of such cells in inflamed muscle tissues compared to their wild type counterparts at day 1 and day 2 post injury (Figure 2 D, F). In comparison with the Mcl1ΔMyelo mice, we observed an elevated number of $F4/80^+$ $Ly6C^{low}$ macrophages in the WT animals at day 3 post injury (Figure 2 D, G). The situation regarding eosinophil granulocyte numbers was opposite to that of other measured myeloid cell types. We regularly observed and measured an elevated number of eosinophils in injured muscles of Mcl1ΔMyelo mice – especially from day 3 p.i. – but the significance of these differences were above the generally accepted probability value (Figure 2 B, E).

**Elevated T cell number in the injured muscle of Mcl1ΔMyelo animals**

At the third day post injury, the $CD45^+$ leukocyte number was similar in the muscles of the two different examined mouse strains (Figure 2 A). The measured differences in myeloid cell numbers showed a discrepancy with the measured $CD45^+$ leukocyte numbers. T cells also take part in the differentiation process of the macrophages in various functional states. We observed remarkable differences in T cell numbers between WT and Mcl1ΔMyelo mice (Figure 3).

We counted an elevated number of both alpha-beta (αβ) and gamma-delta (γδ) T cells within the injured muscle samples of neutrophil deficient Mcl1ΔMyelo mice by flow cytometry (Supplementary figure S4). The differences could be seen as early as day 1 p.i. The T cell numbers in muscles peaked

around day 3 or day 4 p.i. More than 10× higher T cell number could be measured the in the injured muscles of the Mcl1ΔMyelo mice at day 3 p.i., and the differences could be observed even at day 7 p.i. The ratio of the γδ T cell population was elevated in injured tissue both in WT and Mcl1ΔMyelo mice compared to the situation normally found within blood circulation. The γδ T cell number could almost reach the number of αβ T cells within injured muscle tissues (Figure 3 C).

**General differences between WT and Mcl1ΔMyelo mice**

We tried to reveal the cause of the remarkable T cell number differences shown in injured muscles of WT and Mcl1ΔMyelo mice. Therefore, we examined various known and non-described properties of the Mcl1Δmyelo mice.

As inflammatory conditions could influence various cell types and different components of the immune system, we sought traces of pre-existing inflammatory conditions in Mcl1ΔMyelo mice. We measured an increased serum amyloid P component (SAP) concentration in sera of Mcl1ΔMyelo mice (Figure 4 A). SAP belongs to the pentraxin family and is one of the major positive acute-phase proteins in mice [38]. The presence of elevated SAP levels in circulation indicates inflammatory conditions in the body. We assume that the absence of neutrophil granulocytes can make the gastrointestinal tract or the epidermis vulnerable against infections caused by normal, commensal microbiota. Gastrointestinal inflammatory conditions could negatively influence the nutritional function of the gut. These circumstances could be a reasonable explanation for both the increased SAP level and low body weight of the Mcl1ΔMyelo mice (Figure 4 B, C) [3].

**Altered cellular composition in the bone marrow of Mcl1ΔMyelo mice**

We observed visible colour differences in the femoral and tibial bones between the WT and the Mcl1ΔMyelo mice (Figure 5 A). The bone colour of the Mcl1ΔMyelo mice is paler compared to the WT animals. The different colour could imply differences in either the volume or composition of the encompassed bone marrow. Indeed, after isolating the bone marrows from the femoral bones of the WT and Mcl1ΔMyelo mice, we observed color differences, but there was no obvious difference between the volumes of the isolated bone marrow samples (Figure 5 B). The $CD45^{+}$ leukocyte cell numbers in the bone marrow were not significantly different (Figure 6 B).

We assumed that the discrepancy in T cell numbers could be connected with altered lymphoid cell development of the Mcl1ΔMyelo mice. To clarify this, we have investigated the cellular composition of the bone marrow both in WT and Mcl1ΔMyelo mice using flow cytometry (Figure 6).

After cytometric staining procedures, we identified and counted the number of common lymphoid precursor cells (CLP) and common myeloid precursor cells (CMP), according a well-established protocol, involving the use of several cell type markers (Supplementary figure S5) [39-41]. We did not detect significant differences in the number of these precursor cells in the bone marrow of WT and Mcl1ΔMyelo mice (Figure 6 A).

As expected from the Mcl1ΔMyelo mouse model, there was a large difference in the development of neutrophil granulocytes. The bone marrow of WT animals contained a large number of conventional $CD11b^{+}$ $Ly6G^{++}$ $CD125^{+}$ neutrophil granulocytes (Figure 6 D, F). The development of neutrophil granulocytes is obstructed by Mcl1 deficiency within Mcl1ΔMyelo mice [2]. This results in the accumulation of a large number atypical $CD11b^{+}$ $Ly6G^{low}$ $CD125^{+}$ cells in the bone marrow, and only a scarce number of conventional $Ly6G^{++}$ neutrophil granulocytes can be observed (Figure 6 D, F). This phenomenon can be found, but was not emphasized, in a previous study [2] with Mcl1ΔMyelo ($Mcl1^{-/-}$) mice, using the Ly6G/Ly6C specific Gr-1 monoclonal antibody. As it is difficult to assess the

boundaries of underdeveloped atypical neutrophil populations on flow cytometry plots (Figure 6 F), we compared the ratio of intermediate/low Ly6G expressing atypical neutrophil numbers to conventional Ly6G$^{++}$ neutrophil cell numbers to emphasize the difference (Figure 6 E) (Supplementary figure S7). We did not detect significant differences in the numbers of CD11b$^{+}$ Ly6C$^{+}$ monocytoid cells, and there were no differences in the numbers of developed CD11b$^{+}$ SiglecF$^{+}$ eosinophil granulocytes either (Figure 6 D). We confirmed a decreased number of CD19$^{+}$ B cells in the bone marrow of Mcl1ΔMyelo mice (Figure 6 C), which was also mentioned elsewhere [3].

Surprisingly large differences were observed in the numbers of the erythroid cell types. The bone marrow of Mcl1ΔMyelo mice contains significantly fewer erythrocytes, reticulocytes, and nucleated erythroblasts compared to WT animals (Figure 7 A, B). These populations were identified by the presence of Ter119 erythrocyte marker and nucleic acid content of the cells (Supplementary figure S8). The low number of the erythroid cells within bone marrow could explain pale colour of Mcl1ΔMyelo femoral and tibial bones.

**Comparison of blood cells**

As described elsewhere [2, 3], with the exception of the neutrophil granulocytes, there were no differences in the composition of the main cell populations between the blood of WT and the blood of Mcl1ΔMyelo mice, including the number of eosinophil granulocytes. We did not find significant differences in the numbers of large T cell subpopulations either (Figure 8 A). We could not show differences in the number of erythrocytes (Figure 8 B), but we found an elevated number of reticulocytes in the blood of Mcl1ΔMyelo mice (Figure 8 C).

**Altered cellular composition in the spleen of Mcl1ΔMyelo mice**

We observed remarkable differences in the size of the spleen between WT and Mcl1ΔMyelo animals (Figure 9 A). We observed splenomegaly of Mcl1ΔMyelo mice on several occasions. We calculated the ratio of spleen mass to body mass for several WT and Mcl1ΔMyelo mice and found significant differences (Figure 9 B).

The observed increased size and weight imply differences in the cellular composition of the spleen. After flow cytometric investigation of spleen cells from WT and Mcl1ΔMyelo mice, we could not show significant differences in the numbers of the CD45$^{+}$ leukocytes (Figure 9 D), CD11b$^{+}$ Ly6C$^{++}$ monocytoid cells, CD11b$^{+}$ F4/80$^{+}$ macrophages (Figure 9 E), or SiglecF$^{+}$ eosinophil granulocytes (Figure 9 F). There were no differences in the number of αβ- and γδ T cell populations either (Figure 9 G). We showed a higher number of CD19$^{+}$ B-lymphocytes in the spleen cell suspension from Mcl1ΔMyelo mice (Figure 9 H).

Surprisingly we found a high amount of atypical CD11b$^{+}$ Ly6G$^{low}$ neutrophil granulocytes in the spleen of the Mcl1ΔMyelo mice (Figure 9 C) as was also seen in bone marrow (Figure 6 F). This was also observed elsewhere using CD11b(Mac-1) and Ly6G/Ly6C specific Gr-1 antibodies [2].The number of CD11b$^{+}$ Ly6G$^{high}$ CD125$^{+}$ conventional neutrophil granulocytes was higher in the spleen of the WT animals compared to Mcl1ΔMyelo mice, but their absolute numbers were rather low in both WT and Mcl1ΔMyelo mice (Figure 9 F).

The presence of atypical neutrophils suggests that their development could also proceed in the spleen of Mcl1ΔMyelo mice. Therefore, we examined the presence of common lymphoid and common myeloid precursor cells in spleen cell suspension (Supplementary figure S6), and showed a significantly higher number of CMP cells in the spleen of Mcl1ΔMyelo mice (Figure 9 I). As CMP cells could give rise to precursors of erythroid cells, we also investigated the erythroid cells in the spleen

(Supplementary figure S8). We measured an excess of nucleated erythroblastoid cells in three samples from Mcl1ΔMyelo mice, with near significance (p=0.07) (Figure 7 C, D). If we considered the ratio of nucleated erythroblasts to mature erythrocytes, we obtained significant differences (Figure 7 E). These findings may indicate extramedullary haematopoiesis in the spleen of Mcl1ΔMyelo mice.

## Discussion

In this neutrophil granulocyte-deficient mouse model, several changes were observed at both the cellular and organ levels. The most obvious change was the difference in the regeneration process of muscle injuries. However, other unexpected differences were also seen in the spleen and bones of neutrophil-deficient animals.

We observed paler femoral and tibial bones, as well as enlarged spleen size in the neutrophil deficient mice. It is thought that the increased demand for neutrophils may increase neutrophil production in the bone marrow. This demand can be induced in response to subacute commensal microbe-mediated inflammations of varying severity, which also induce elevated levels of acute phase proteins (Figure 4 A). We suggest that the increased production of neutrophil granulocytes and the accumulation of apoptotic neutrophil precursors in the bone marrow limit erythrocyte production, indirectly resulting in erythroid cell type-specific bone marrow insufficiency. Low erythrocyte numbers or hypoxia induce extramedullary erythropoiesis [42] in the spleen of the Mcl1ΔMyelo mice. The increased number of CMP in the spleen (Figure 9 I) give rise not only the erythrocytes, but also to precursors of neutrophils. In the absence of Mcl1, the emerging immature atypical Ly6G$^{low}$ neutrophils (Figure 9 C) probably die inside the spleen, similarly to what was seen in the case of the bone marrow (Figure 6 E, F) [2]. The consequence of the increased cell production manifests itself in the visible morphology of the spleen as splenomegaly (Figure 9 A) [43, 44].

The absence of immigrating neutrophil granulocytes in the injured muscle tissue could influence the further inflammatory and regeneration-prone response of the immune system. Our experiments support the role of neutrophil granulocytes in muscle regeneration at cellular level. A lower number of tissue-immigrating Ly6C$^{++}$ monocytoid cells were observed in processed muscle suspension from Mcl1ΔMyelo mice during the first days after tissue injury (Figure 2 F). The low number of these monocytoid cells may be attributed to missing chemotactic factor production in the absence of neutrophils. The production of inflammatory cytokines derived from monocytoid Ly6C$^{++}$ macrophages (e.g. TNF, IL-6), which could increase the proliferation of muscle stem cells (satellite cells) [45, 46] could be unaltered in Mcl1ΔMyelo mice. As explanation, we suggest that necrotic tissue is present for extended period in the absence of neutrophils (Figure 1 B1 insert). This confers strong activation stimuli for monocytoid macrophages during the first days after injury, compensating for their decreased number, especially without the presence of apoptotic neutrophils that could otherwise confer anti-inflammatory effects through efferocytosis [47]. In the absence of neutrophils, proliferating fibro-adipogenic precursor cells also participate in phagocytosis of necrotic debris, potentially skewing their differentiation towards adipocytes, as seen on our histopathology images (Figure 1 B).

The appearance of F4/80$^{+}$ Ly6C$^{low}$ macrophages, associated with anti-inflammatory and regenerative functions [29], was delayed and their numbers were lower in the regenerating muscles from Mcl1ΔMyelo mice (Figure 2 G). The tissue differentiation process, which depends on cytokine producing M2-like resolving macrophages, is altered (Figure 1 B).

A surprisingly high number of T cells were observed in injured muscle from Mcl1ΔMyelo mice (Figure 3). As there were no differences in T cell numbers in the blood or spleen between wild-type and

Mcl1ΔMyelo mice (Figure 8 A, Figure 9 G), the increased T cell numbers in injured muscles may be connected with altered chemotaxis of T cells in neutrophil deficient animals. We may explain this observation by a hypothetic mechanism: In wild type animals, neutrophils extravasate into injured tissues in large numbers, driven by various chemotactic factors released from injured tissue [15-17]. During neutrophil granulocyte extravasation, interactions occur between various receptors used for chemotaxis and cell activation and their cognate chemotactic ligands. The receptors bind and later internalise endothelial surface-adhered chemotactic ligands during this process, so in high numbers, extravasating neutrophils "consume" the chemotactic factors. In Mcl1ΔMyelo mice, other cell types – e.g., effector T helper cells of Th2 phenotype or subpopulations of gamma-delta (γδ) T cells – armed with similar tissue injury sensor receptors or chemokine receptors are attracted to the site of tissue injury in high numbers instead of missing neutrophils.

An alternative explanation would be the absence of arginase enzyme activity without the presence of neutrophils [25] in injured tissue, which may favour the proliferation of extravasating T cells [48].

T cells can influence macrophage activation and function in various ways. Activated effector T cells in tissue produce cytokines that polarise or reprogram macrophages [49]. Cell-cell contacts between T cells and macrophages during antigen presentation can induce the activation of both cell types. Recognition of stress indicator molecules appearing on the surface of macrophages and other tissue cells during stress response can activate non-conventional T cells, such as subtypes of γδ T cells. The ratio of γδ T cells is strongly increased in the injured tissues (Figure 3 C) compared to blood or spleen. This increase was seen both in wild-type and Mcl1ΔMyelo mice (Figure 3 C). However, in Mcl1ΔMyelo mice, the absolute numbers of both αβ- and γδ T cells were strongly increased (Figure 3 B, C).

It is known that γδ T cells participate in the regeneration process of various tissues. Skin γδ T cells produce growth factors (e.g., insulin-like growth factor-1 IGF1) [50, 51] during wound healing. There are data on the role of IL-17 producing, neutrophil-recruiting γδ T cells in CTX induced muscle injury [52]. The number of T cells peaks around day 3 post injury (Figure 3 B) in muscles (as was also mentioned elsewhere [52]) and neutrophil granulocytes disappear around the same time (Figure 2 C). This weakens the hypothesis about the role of these IL-17 producing T cells in recruiting neutrophil granulocytes to muscle injury and suggests other immunoregulatory and indirect tissue regeneration roles.

We have shown that the number of eosinophil granulocytes similarly increased with T cells in injured muscles of Mcl1ΔMyelo mice. Eosinophils can also be recruited by danger signals released during tissue injury [53], and this recruitment may be more effective without the presence of neutrophils. The presence of Th2-like T cells appearing in various intense tissue injuries could produce chemotactic factors that also attract eosinophils and vice versa [54]. Cytokines released by eosinophils and immigrating T cells (e.g., IL-4 production) may participate in the differentiation of M2-like resolving macrophages and act directly on muscle tissue precursor cells [55].

We believe that the elevated number of T cells in the injured muscles of Mcl1ΔMyelo mice may compensate for the immune modulatory functions of apoptotic neutrophil granulocytes through their own immunomodulatory functions. Together with eosinophil granulocytes, they could attract, activate, and polarise macrophages in injured muscle tissue to promote tissue repair.

Nevertheless, based on our histopathology findings, it is reasonable to suggest that the overall pattern of neutrophil-deficient inflammation in Mcl1ΔMyelo mice is insufficient for complete muscle resolution, even in the presence of increased numbers of lymphoid cells. The elevated number of adipocytes indicates an altered regeneration process.

The complex immunological and physiological changes manifested in neutrophil deficient Mcl1ΔMyelo animals during muscle injury hinder understanding of the direct role of neutrophils in the process. However, the high number of T cells appearing in injured muscles may provide an excellent opportunity for investigating T cell function in muscle regeneration.

## Acknowledgements:

Maintenance of the mouse colonies and animal husbandry were performed in the Laboratory Animal Faculty, Life Science Building, University of Debrecen. We gratefully acknowledge the technical assistance of Dávid Deák, Adrienn Gyöngyösi, György Hajas, and Katalin Orosz-Tóth

**Institutional Review Board Statement:** The study was conducted according to the guidelines of the Declaration of Helsinki and approved by the Institutional Ethics Committee of University Debrecen under the protocol code of 16/2019/DEMÁB.

**Funding:** This study was supported by the National Research, Development and Innovation Office, Hungary, grant number K 125477

**Informed Consent Statement:** Not applicable

**Conflicts of Interest:** The authors declare no conflict of interest.

**Author Contributions:**

Conceptualization: H.H. and P.G.; Methodology: H.H., A.P., P.G., T.V., B.D., A.M.; Formal analysis: H.H., P.G., B.D.; Investigations: H.H., P.G., T.V., B.D.; Writing—Original draft preparation: H.H., P.G.; Writing—Review and editing: P.G., L.N., A.M., B.D.; Visualization: H.H., P.G., B.D.; Supervision: P.G.; Project administration: P.G.; Resources: A.M., A.P., T.V.; Funding acquisition: T.V., L.N.
All authors reviewed the results and approved the final version of the manuscript.

**Data Availability Statement:**

The data presented in this study are available upon request from the corresponding author.

**Supporting information:** Supplementary figures - Figure S1-S8 – can be found within the "Supplementary Figures.pdf" file.



## References

1. McLellan, M.A., N.A. Rosenthal, and A.R. Pinto, *Cre-loxP-Mediated Recombination: General Principles and Experimental Considerations.* Curr Protoc Mouse Biol, 2017. **7**(1): p. 1-12.
2. Dzhagalov, I., A. St John, and Y.W. He, *The antiapoptotic protein Mcl-1 is essential for the survival of neutrophils but not macrophages.* Blood, 2007. **109**(4): p. 1620-6.
3. Csepregi, J.Z., et al., *Myeloid-Specific Deletion of Mcl-1 Yields Severely Neutropenic Mice That Survive and Breed in Homozygous Form.* J Immunol, 2018. **201**(12): p. 3793-3803.
4. Mocsai, A., *Diverse novel functions of neutrophils in immunity, inflammation, and beyond.* J Exp Med, 2013. **210**(7): p. 1283-99.
5. Nathan, C., *Neutrophils and immunity: challenges and opportunities.* Nat Rev Immunol, 2006. **6**(3): p. 173-82.
6. Soehnlein, O., C. Weber, and L. Lindbom, *Neutrophil granule proteins tune monocytic cell function.* Trends Immunol, 2009. **30**(11): p. 538-46.

7. van Gisbergen, K.P., et al., *Neutrophils mediate immune modulation of dendritic cells through glycosylation-dependent interactions between Mac-1 and DC-SIGN.* J Exp Med, 2005. **201**(8): p. 1281-92.
8. Wittamer, V., et al., *Neutrophil-mediated maturation of chemerin: a link between innate and adaptive immunity.* J Immunol, 2005. **175**(1): p. 487-93.
9. Beauvillain, C., et al., *Neutrophils efficiently cross-prime naive T cells in vivo.* Blood, 2007. **110**(8): p. 2965-73.
10. Puga, I., et al., *B cell-helper neutrophils stimulate the diversification and production of immunoglobulin in the marginal zone of the spleen.* Nat Immunol, 2011. **13**(2): p. 170-80.
11. Baghdadi, M.B. and S. Tajbakhsh, *Regulation and phylogeny of skeletal muscle regeneration.* Dev Biol, 2018. **433**(2): p. 200-209.
12. Tidball, J.G., *Regulation of muscle growth and regeneration by the immune system.* Nat Rev Immunol, 2017. **17**(3): p. 165-178.
13. Tedesco, F.S., et al., *Repairing skeletal muscle: regenerative potential of skeletal muscle stem cells.* J Clin Invest, 2010. **120**(1): p. 11-9.
14. Hardy, D., et al., *Comparative Study of Injury Models for Studying Muscle Regeneration in Mice.* PLoS One, 2016. **11**(1): p. e0147198.
15. Chen, Y., et al., *ATP release guides neutrophil chemotaxis via P2Y2 and A3 receptors.* Science, 2006. **314**(5806): p. 1792-5.
16. de Oliveira, S., et al., *ATP modulates acute inflammation in vivo through dual oxidase 1-derived H2O2 production and NF-kappaB activation.* J Immunol, 2014. **192**(12): p. 5710-9.
17. Huang, C. and P. Niethammer, *Tissue Damage Signaling Is a Prerequisite for Protective Neutrophil Recruitment to Microbial Infection in Zebrafish.* Immunity, 2018. **48**(5): p. 1006-1013 e6.
18. Yang, D., Z. Han, and J.J. Oppenheim, *Alarmins and immunity.* Immunol Rev, 2017. **280**(1): p. 41-56.
19. Tecchio, C., A. Micheletti, and M.A. Cassatella, *Neutrophil-derived cytokines: facts beyond expression.* Front Immunol, 2014. **5**: p. 508.
20. Yang, W. and P. Hu, *Skeletal muscle regeneration is modulated by inflammation.* J Orthop Translat, 2018. **13**: p. 25-32.
21. Lepper, C., T.A. Partridge, and C.M. Fan, *An absolute requirement for Pax7-positive satellite cells in acute injury-induced skeletal muscle regeneration.* Development, 2011. **138**(17): p. 3639-46.
22. Sambasivan, R., et al., *Pax7-expressing satellite cells are indispensable for adult skeletal muscle regeneration.* Development, 2011. **138**(17): p. 3647-56.
23. Kovtun, A., et al., *Neutrophils in Tissue Trauma of the Skin, Bone, and Lung: Two Sides of the Same Coin.* J Immunol Res, 2018. **2018**: p. 8173983.
24. Peiseler, M. and P. Kubes, *More friend than foe: the emerging role of neutrophils in tissue repair.* J Clin Invest, 2019. **129**(7): p. 2629-2639.
25. Bryk, J.A., et al., *Nature of myeloid cells expressing arginase 1 in peripheral blood after trauma.* J Trauma, 2010. **68**(4): p. 843-52.
26. Arnold, L., et al., *Inflammatory monocytes recruited after skeletal muscle injury switch into antiinflammatory macrophages to support myogenesis.* J Exp Med, 2007. **204**(5): p. 1057-69.
27. Giannakis, N., et al., *Dynamic changes to lipid mediators support transitions among macrophage subtypes during muscle regeneration.* Nat Immunol, 2019. **20**(5): p. 626-636.
28. Kim, J. and J. Lee, *Role of transforming growth factor-beta in muscle damage and regeneration: focused on eccentric muscle contraction.* J Exerc Rehabil, 2017. **13**(6): p. 621-626.
29. Varga, T., et al., *Macrophage PPARgamma, a Lipid Activated Transcription Factor Controls the Growth Factor GDF3 and Skeletal Muscle Regeneration.* Immunity, 2016. **45**(5): p. 1038-1051.

30. Jacquot, S., et al., *Optimizing PCR for Mouse Genotyping: Recommendations for Reliable, Rapid, Cost Effective, Robust and Adaptable to High-Throughput Genotyping Protocol for Any Type of Mutation.* Curr Protoc Mouse Biol, 2019. **9**(4): p. e65.
31. Guardiola, O., et al., *Induction of Acute Skeletal Muscle Regeneration by Cardiotoxin Injection.* J Vis Exp, 2017(119).
32. Kruisbeek, A.M., *Isolation of mouse mononuclear cells.* Curr Protoc Immunol, 2001. **Chapter 3**: p. Unit 3 1.
33. Liu, X. and N. Quan, *Immune Cell Isolation from Mouse Femur Bone Marrow.* Bio Protoc, 2015. **5**(20).
34. Parasuraman, S., R. Raveendran, and R. Kesavan, *Blood sample collection in small laboratory animals.* J Pharmacol Pharmacother, 2010. **1**(2): p. 87-93.
35. Fleming, T.J., M.L. Fleming, and T.R. Malek, *Selective Expression of Ly-6g on Myeloid Lineage Cells in Mouse Bone-Marrow - Rb6-8c5 Mab to Granulocyte-Differentiation Antigen (Gr-1) Detects Members of the Ly-6 Family.* Journal of Immunology, 1993. **151**(5): p. 2399-2408.
36. Sasmono, R.T., et al., *Mouse neutrophilic granulocytes express mRNA encoding the macrophage colony-stimulating factor receptor (CSF-1R) as well as many other macrophage-specific transcripts and can transdifferentiate into macrophages in vitro in response to CSF-1.* J Leukoc Biol, 2007. **82**(1): p. 111-23.
37. Daley, J.M., et al., *Use of Ly6G-specific monoclonal antibody to deplete neutrophils in mice.* J Leukoc Biol, 2008. **83**(1): p. 64-70.
38. Bottazzi, B., et al., *The pentraxins PTX3 and SAP in innate immunity, regulation of inflammation and tissue remodelling.* J Hepatol, 2016. **64**(6): p. 1416-27.
39. Akashi, K., et al., *A clonogenic common myeloid progenitor that gives rise to all myeloid lineages.* Nature, 2000. **404**(6774): p. 193-7.
40. Challen, G.A., et al., *Mouse hematopoietic stem cell identification and analysis.* Cytometry A, 2009. **75**(1): p. 14-24.
41. Kondo, M., I.L. Weissman, and K. Akashi, *Identification of clonogenic common lymphoid progenitors in mouse bone marrow.* Cell, 1997. **91**(5): p. 661-72.
42. Cenariu, D., et al., *Extramedullary Hematopoiesis of the Liver and Spleen.* J Clin Med, 2021. **10**(24).
43. Chiu, S.C., et al., *Extramedullary hematopoiesis (EMH) in laboratory animals: offering an insight into stem cell research.* Cell Transplant, 2015. **24**(3): p. 349-66.
44. Yamamoto, K., et al., *Extramedullary hematopoiesis: Elucidating the function of the hematopoietic stem cell niche (Review).* Mol Med Rep, 2016. **13**(1): p. 587-91.
45. Bentzinger, C.F., et al., *Cellular dynamics in the muscle satellite cell niche.* EMBO Rep, 2013. **14**(12): p. 1062-72.
46. Karalaki, M., et al., *Muscle regeneration: cellular and molecular events.* In Vivo, 2009. **23**(5): p. 779-96.
47. Lawrence, S.M., R. Corriden, and V. Nizet, *How Neutrophils Meet Their End.* Trends Immunol, 2020. **41**(6): p. 531-544.
48. Werner, A., et al., *Reconstitution of T Cell Proliferation under Arginine Limitation: Activated Human T Cells Take Up Citrulline via L-Type Amino Acid Transporter 1 and Use It to Regenerate Arginine after Induction of Argininosuccinate Synthase Expression.* Front Immunol, 2017. **8**: p. 864.
49. Orecchioni, M., et al., *Macrophage Polarization: Different Gene Signatures in M1(LPS+) vs. Classically and M2(LPS-) vs. Alternatively Activated Macrophages.* Front Immunol, 2019. **10**: p. 1084.
50. Hu, W., et al., *Skin gammadelta T Cells and Their Function in Wound Healing.* Front Immunol, 2022. **13**: p. 875076.
51. Mills, R.E., et al., *Defects in skin gamma delta T cell function contribute to delayed wound repair in rapamycin-treated mice.* J Immunol, 2008. **181**(6): p. 3974-83.

52. Mann, A.O., et al., *IL-17A-producing gammadeltaT cells promote muscle regeneration in a microbiota-dependent manner.* J Exp Med, 2022. **219**(5).
53. Long, H., et al., *A Player and Coordinator: The Versatile Roles of Eosinophils in the Immune System.* Transfus Med Hemother, 2016. **43**(2): p. 96-108.
54. Spencer, L.A. and P.F. Weller, *Eosinophils and Th2 immunity: contemporary insights.* Immunol Cell Biol, 2010. **88**(3): p. 250-6.
55. Heredia, J.E., et al., *Type 2 innate signals stimulate fibro/adipogenic progenitors to facilitate muscle regeneration.* Cell, 2013. **153**(2): p. 376-88.

## Figure legends

**Figure 1.** Typical microscopic histopathological images of the Hematoxylin-Eosin (HE)-stained cryosection tissue samples obtained from CTX-induced tibial anterior (TA) muscle damage at day 8 post-injury (p.i.). **A1-A2** shows TA muscles of WT mice and **B1-B2** shows TA muscles of Mcl1ΔMyelo mice, respectively. All tissue samples show comparable muscle regeneration at this time, characterized by the presence of newly formed myofibers with centrally located nuclei or multinucleated (fused) myocytes. The cross sections of the newly formed myofibers are visibly larger, as compared to the normal, unaffected ones (see **A2**, insert). CTX-induced skeletal muscle injuries of WT mice with intact neutrophils show a coordinated regeneration at day 8 p.i. (**A1**-**A2**) exhibiting decreased perimyseal cellular activities. Only few macrophage type mononuclear inflammatory elements remain within the septa (dark blue arrows). CTX-damaged muscles of neutrophil-deficient Mcl1ΔMyelo mice (**B1**-**B2**) show protracted, incomplete and irregular regeneration with remnants of non-eliminated necrotic tissue debris (**B1** insert) and a significantly increased number of mononuclear cells with small, round dark nuclei and narrow cytoplasmic rims (**B2**, green arrows), identified as lymphocytes. Additionally, among these inflammatory cells, there are many non-vital (dead) cells with no nuclear staining (a few indicated by the the green arrowheads, **B2**). This incomplete regenerative process is accompanied by an increased number of intramuscular adipocytes (light blue arrows, compare **B1** with **A1**). Scale bars on all images: 100 µm.

**Figure 2.** Comparison of different leukocyte population numbers between WT and Mcl1ΔMyelo mice in the injured muscles. (A) Comparison of the numbers of living $CD45^+$ leukocytes at different indicated time points post injury (p.i.). (B) Flow cytometric measurements of living $CD45^+$ $CD11b^+$ $SiglecF^+$ cells (eosinophils) and living $CD45^+$ $CD11b^+$ $Ly6G^+$ cells (neutrophils) at days 1 p.i. (C) Comparison of neutrophil granulocyte numbers at day 1, 2, and 3 p.i. (D) Flow cytometric measurements of living $CD45^+$ $CD11b^+$ $SiglecF^{negative}$ $Ly6G^{negative}$ macrophage populations at day 1 p.i. (E) Comparison of the eosinophil granulocyte numbers at day 1, 2, 3 and 7 p.i. (F) Comparison of $Ly6C^{++}$ monocytoid macrophage numbers at indicated time points p.i. (G) Comparison of $F4/80^+$ $Ly6C^{low}$ monocytoid macrophage numbers at indicated time points p.i. Sample number n=5. Significance labels: * $p<0.05$; ** $p<0.01$; *** $p<0.002$.

**Figure 3.** T cells found in the injured tissues of WT and Mcl1ΔMyelo mice according to their $CD45^+$ $CD90^+$ $CD3^+$ expression. (A) Flow cytometric measurements of living αβ- and γδ T cells at day 3 post injury in WT and Mcl1ΔMyelo mice. (B) Living $CD3^+$ T cell numbers measured in injured tissues of WT and Mcl1ΔMyelo mice at the indicated time points post-injury. (C) The number of αβ- and γδ T cells

at indicated time points post-injury in injured tissue. At day 1 p.i, we had measured borderline significance: p=0.055 in the αβ T cell- and p=0.053 in the γδ T cell populations. Sample numbers: n=3 at day 1 and day 7; n=6 at day 3. Significance labels: * p<0.05; ** p<0.01.

**Figure 4.** Comparison of blood plasma acute phase proteins and body weight of WT and Mcl1ΔMyelo mice. (A) Serum amyloid P (pentraxin 2) level in plasma of WT and Mcl1ΔMyelo mice (n=9). Comparison of average weight of WT and Mcl1ΔMyelo mice within the 10 - and 14-week old male (B) (n=4) and female (C) (n=3) mouse groups. Significance indicators: * p<0.05; ** p<0.01; *** p<0.002.

**Figure 5.** Photograph of tibial bones, femoral bones and isolated bone marrow of WT and Mcl1ΔMyelo mice. (A) Tibial bones (left pairs within groups) and femoral bones (right pairs within groups) of WT and Mcl1ΔMyelo mice. (B) Bone marrows obtained from femoral bones of WT and Mcl1ΔMyelo mice after centrifugation in sample tubes.

**Figure 6.** Comparison of different leukocyte populations between WT and Mcl1ΔMyelo mice found in their bone marrow. (A) Comparison of common lymphoid precursor (CLP) numbers and the common myeloid precursor cell (CMP) numbers within different animals (n=5). (B) Comparison of living $CD45^+$ leukocyte numbers (n=4). (C) Comparison of living $CD19^+$ B cells numbers (n=4). (D) Comparison of living $CD11b^+$ $Ly6C^+$ monocytoid cell numbers, conventional living $CD11b^+$ $Ly6G^+$ neutrophil numbers, and the living $CD11b^+$ $SiglecF^+$ eosinophil granulocyte numbers (n=3). (E) Ratio of atypical $Ly6G^{low}$ neutrophils to conventional mature $Ly6G^{++}$ neutrophil granulocytes. (F) Flow cytometric representation of $CD45^+$ $CD11b^+$ neutrophil granulocytes within bone marrow of WT and Mcl1ΔMyelo mice. More $Ly6G^{++}$ cells can be observed in the case of the WT animals. Bone marrow of Mcl1ΔMyelo mice contains high number of atypical or immature $Ly6G^{low}$ neutrophils. CD125 is the alpha chain of the IL-5 receptor complex. Significance indicators: * p<0.05; *** p<0.002.

**Figure 7.** Erythroid cell types within bone marrow and spleen of WT and Mcl1ΔMyelo mice. Ter119 is considered an erythroid specific marker. SYTO16 is a cell permeable fluorescent nucleic acid dye. (A) Flow cytometric characterisation of erythroid cell types in bone marrow of WT and Mcl1ΔMyelo mice. (B) Statistical representation of the erythroid cell type numbers within bone marrow of WT and Mcl1ΔMyelo mice (n=5). (C) Flow cytometric characterisation of erythroid cell types in spleen of WT and Mcl1ΔMyelo mice. (D) Statistical representation of erythroid cell type numbers within spleen of WT and Mcl1ΔMyelo mice (n=5). (E) Ratio of the nucleated erythroblast to mature erythrocytes. Nucleated erythroblasts are indicated as “nu-RBC”, reticulocytes indicated as “pre-RBC” and mature red blood cells represented as “RBC”. Significance indicators: * p<0.05; ** p<0.01; *** p<0.002.

**Figure 8.** Comparison of different cellular elements within blood of WT and Mcl1ΔMyelo mice. (A) Cell numbers of main T cell subpopulations within blood of WT and Mcl1ΔMyelo mice. No significant differences were observed (n=3). (B) There is no significant difference in number of mature erythrocytes (RBC) in blood of WT and Mcl1ΔMyelo mice (n=3). (C) Blood of Mcl1ΔMyelo mice has higher number of reticulocytes compared to WT (n=3). Significance indicators: * p<0.05.

**Figure 9.** Differences in the spleen and spleen cells between WT and Mcl1ΔMyelo mice. (A) Splenomegaly was observed on multiple occasions within Mcl1ΔMyelo animals. (B) Statistical comparison of spleen/body weight ratio between WT and Mcl1ΔMyelo animals (n=20). (C) Flow cytometric measurements of living $CD45^+$ $CD11b^+$ cells. Ly6G and CD125 staining help to identify conventional $Ly6G^{++}$ neutrophils in WT animals, and atypical/immature $Ly6G^{low}$ neutrophils in spleen of Mcl1ΔMyelo mice. (D) There are no significant difference in numbers of the living $CD45^+$ leukocytes. (n=3). (E) There are no significant differences in the numbers of monocytoid $Ly6C^+$ cells or $F4/80^+$ $Ly6C^{low}$ macrophages (n=3). (F) There is significantly lower number of conventional $Ly6G^+$ neutrophils in the spleen of Mcl1ΔMyelo mice. There are no significant differences in the numbers of eosinophils (n=3). (G) There are no differences in the numbers of the indicated T cell populations (n=4). (H) There is a significant difference in number of $CD19^+$ B cells (n=4). (I) There is a significant difference in the number of common myeloid precursor cells (CMP) in the spleen, but no significant difference in the number of common lymphoid precursor cells (CLP) (n=5). Significance indicators: * $p<0.05$; ** $p<0.01$.

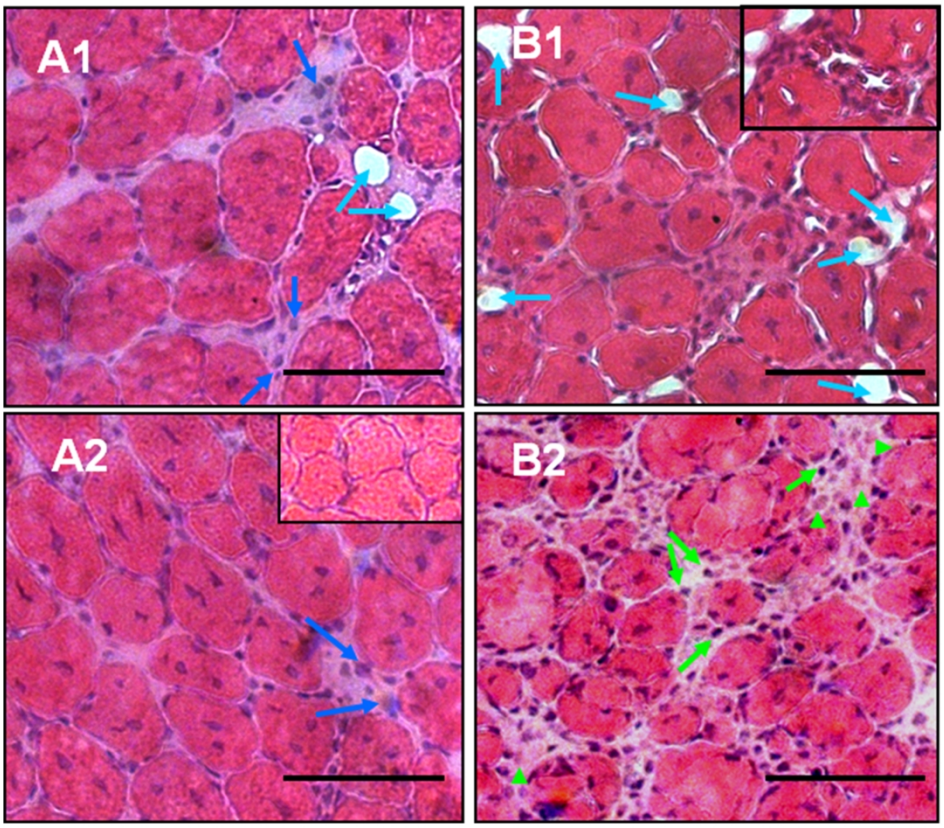


**Figure 1.** Typical microscopic histopathological images of the Hematoxylin-Eosin (HE)-stained cryosection tissue samples obtained from CTX-induced tibial anterior (TA) muscle damage at day 8 post-injury (p.i.). A1-A2 shows TA muscles of WT mice and B1-B2 shows TA muscles of Mcl1ΔMyelo mice, respectively. All tissue samples show comparable muscle regeneration at this time, characterized by the presence of newly formed myofibers with centrally located nuclei or multinucleated (fused) myocytes. The cross sections of the newly formed myofibers are visibly larger, as compared to the normal, unaffected ones (see A2, insert). CTX-induced skeletal muscle injuries of WT mice with intact neutrophils show a coordinated regeneration at day 8 p.i. (A1-A2) exhibiting decreased perimyseal cellular activities. Only few macrophage type mononuclear inflammatory elements remain within the septa (dark blue arrows). CTX-damaged muscles of neutrophil-deficient Mcl1ΔMyelo mice (B1-B2) show protracted, incomplete and irregular regeneration with remnants of non-eliminated necrotic tissue debris (B1 insert) and a significantly increased number of mononuclear cells with small, round dark nuclei and narrow cytoplasmic rims (B2, green arrows), identified as lymphocytes. Additionally, among these inflammatory cells, there are many non-vital (dead) cells with no nuclear staining (a few indicated by the the green arrowheads, B2). This incomplete regenerative process is accompanied by an increased number of intramuscular adipocytes (light blue arrows, compare B1 with A1). Scale bars on all images: 100 μm.

239x209mm (300 x 300 DPI)

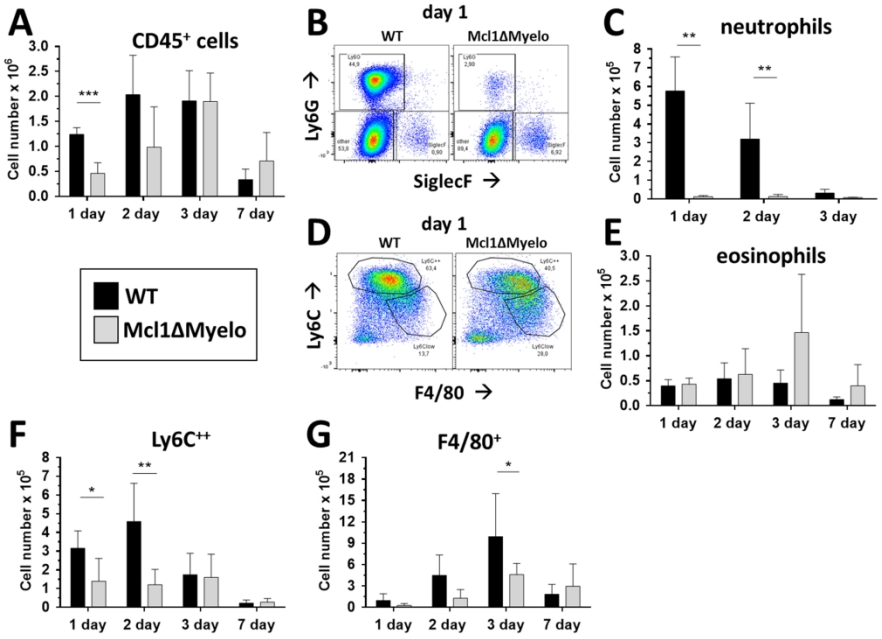


**Figure 2.** Comparison of different leukocyte population numbers between WT and Mcl1ΔMyelo mice in the injured muscles. (A) Comparison of the numbers of living $CD45^+$ leukocytes at different indicated time points post injury (p.i.). (B) Flow cytometric measurements of living $CD45^+$ $CD11b^+$ $SiglecF^+$ cells (eosinophils) and living $CD45^+$ $CD11b^+$ $Ly6G^+$ cells (neutrophils) at days 1 p.i. (C) Comparison of neutrophil granulocyte numbers at day 1, 2, and 3 p.i. (D) Flow cytometric measurements of living $CD45^+$ $CD11b^+$ $SiglecF^{negative}$ $Ly6G^{negative}$ macrophage populations at day 1 p.i. (E) Comparison of the eosinophil granulocyte numbers at day 1, 2, 3 and 7 p.i. (F) Comparison of $Ly6C^{++}$ monocytoid macrophage numbers at indicated time points p.i. (G) Comparison of $F4/80^+$ $Ly6C^{low}$ monocytoid macrophage numbers at indicated time points p.i. Sample number n=5. Significance labels: * $p<0.05$; ** $p<0.01$; *** $p<0.002$.

297x209mm (300 x 300 DPI)

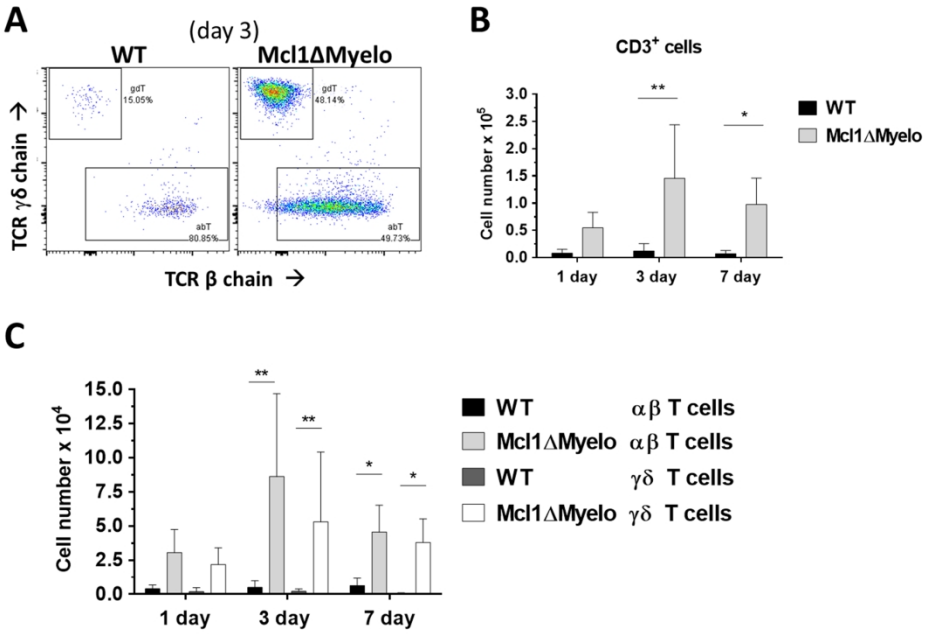


**Figure 3.** T cells found in the injured tissues of WT and Mcl1ΔMyelo mice according to their $CD45^+$ $CD90^+$ $CD3^+$ expression. (A) Flow cytometric measurements of living αβ- and γδ T cells at day 3 post injury in WT and Mcl1ΔMyelo mice. (B) Living $CD3^+$ T cell numbers measured in injured tissues of WT and Mcl1ΔMyelo mice at the indicated time points post-injury. (C) The number of αβ- and γδ T cells at indicated time points post-injury in injured tissue. At day 1 p.i, we had measured borderline significance: p=0.055 in the αβ T cell- and p=0.053 in the γδ T cell populations. Sample numbers: n=3 at day 1 and day 7; n=6 at day 3. Significance labels: * $p<0.05$; ** $p<0.01$.

297x209mm (300 x 300 DPI)

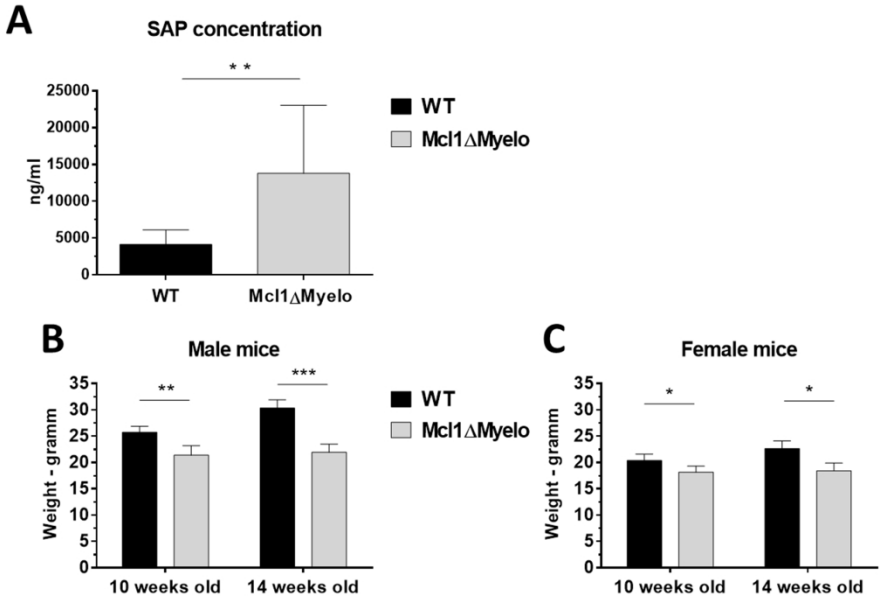


**Figure 4.** Comparison of blood plasma acute phase proteins and body weight of WT and Mcl1ΔMyelo mice. (A) Serum amyloid P (pentraxin 2) level in plasma of WT and Mcl1ΔMyelo mice (n=9). Comparison of average weight of WT and Mcl1ΔMyelo mice within the 10- and 14-week old male (B) (n=4) and female (C) (n=3) mouse groups. Significance indicators: * $p<0.05$; ** $p<0.01$; *** $p<0.002$.

297x209mm (300 x 300 DPI)

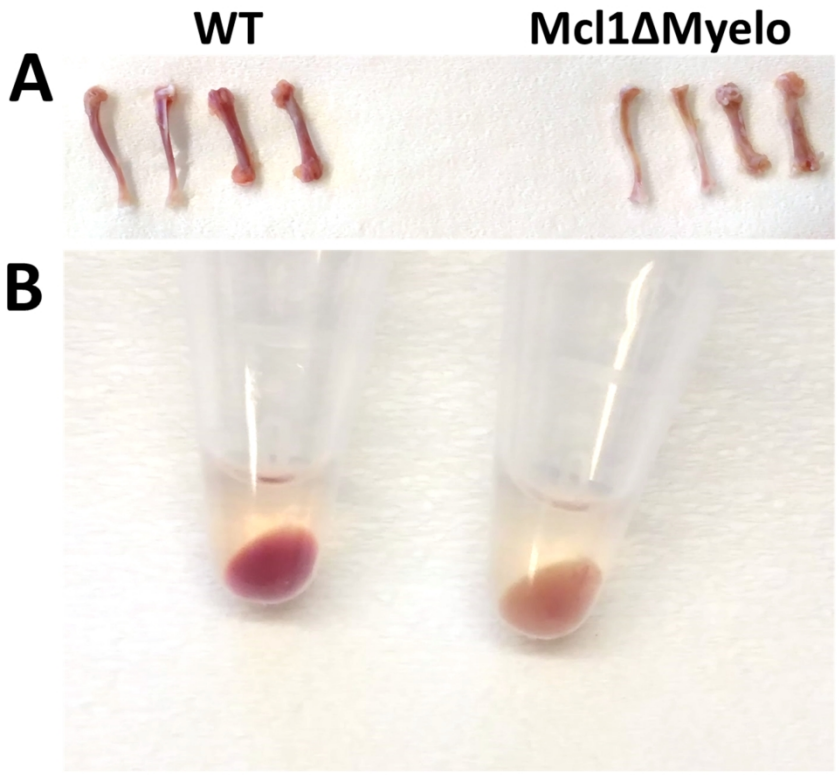


**Figure 5.** Photograph of tibial bones, femoral bones and isolated bone marrow of WT and Mcl1ΔMyelo mice. (A) Tibial bones (left pairs within groups) and femoral bones (right pairs within groups) of WT and Mcl1ΔMyelo mice. (B) Bone marrows obtained from femoral bones of WT and Mcl1ΔMyelo mice after centrifugation in sample tubes.

250x209mm (300 x 300 DPI)

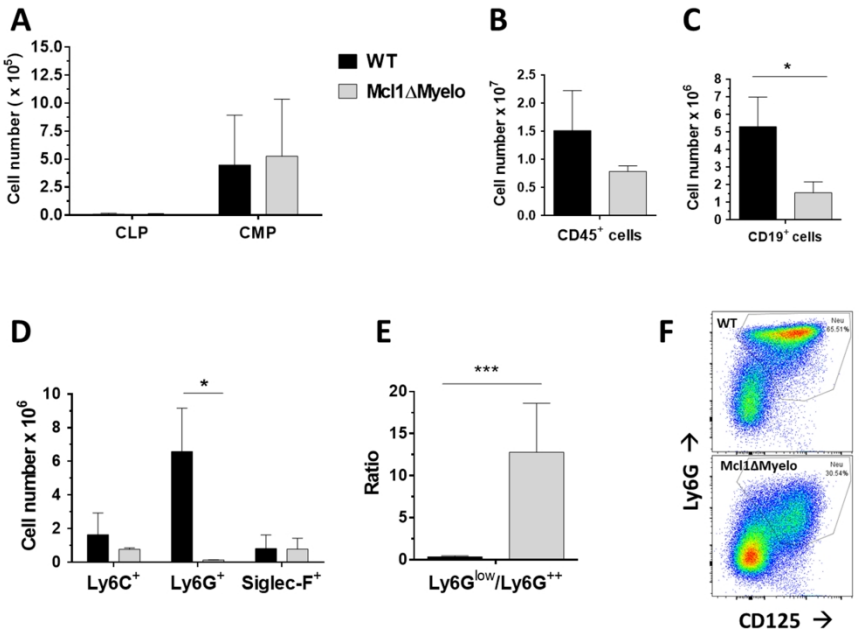


**Figure 6.** Comparison of different leukocyte populations between WT and Mcl1ΔMyelo mice found in their bone marrow. (A) Comparison of common lymphoid precursor (CLP) numbers and the common myeloid precursor cell (CMP) numbers within different animals (n=5). (B) Comparison of living $CD45^+$ leukocyte numbers (n=4). (C) Comparison of living $CD19^+$ B cells numbers (n=4). (D) Comparison of living $CD11b^+$ $Ly6C^+$ monocytoid cell numbers, conventional living $CD11b^+$ $Ly6G^+$ neutrophil numbers, and the living $CD11b^+$ $SiglecF^+$ eosinophil granulocyte numbers (n=3). (E) Ratio of atypical $Ly6G^{low}$ neutrophils to conventional mature $Ly6G^{++}$ neutrophil granulocytes. (F) Flow cytometric representation of $CD45^+$ $CD11b^+$ neutrophil granulocytes within bone marrow of WT and Mcl1ΔMyelo mice. More $Ly6G^{++}$ cells can be observed in the case of the WT animals. Bone marrow of Mcl1ΔMyelo mice contains high number of atypical or immature $Ly6G^{low}$ neutrophils. CD125 is the alpha chain of the IL-5 receptor complex. Significance indicators: * $p<0.05$; *** $p<0.002$.

297x209mm (300 x 300 DPI)

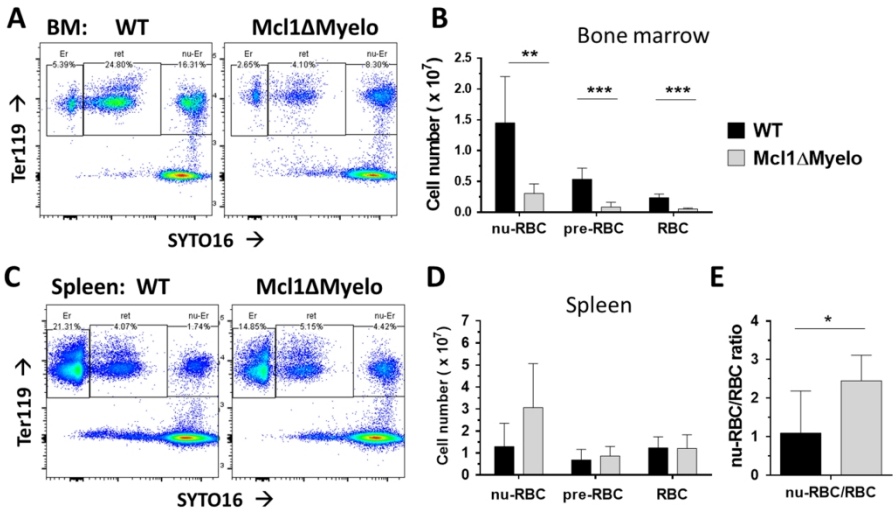


**Figure 7.** Erythroid cell types within bone marrow and spleen of WT and Mcl1ΔMyelo mice. Ter119 is considered an erythroid specific marker. SYTO16 is a cell permeable fluorescent nucleic acid dye. (A) Flow cytometric characterisation of erythroid cell types in bone marrow of WT and Mcl1ΔMyelo mice. (B) Statistical representation of the erythroid cell type numbers within bone marrow of WT and Mcl1ΔMyelo mice (n=5). (C) Flow cytometric characterisation of erythroid cell types in spleen of WT and Mcl1ΔMyelo mice. (D) Statistical representation of erythroid cell type numbers within spleen of WT and Mcl1ΔMyelo mice (n=5). (E) Ratio of the nucleated erythroblast to mature erythrocytes. Nucleated erythroblasts are indicated as "nu-RBC", reticulocytes indicated as "pre-RBC" and mature red blood cells represented as "RBC". Significance indicators: * $p<0.05$; ** $p<0.01$; *** $p<0.002$.

297x209mm (300 x 300 DPI)

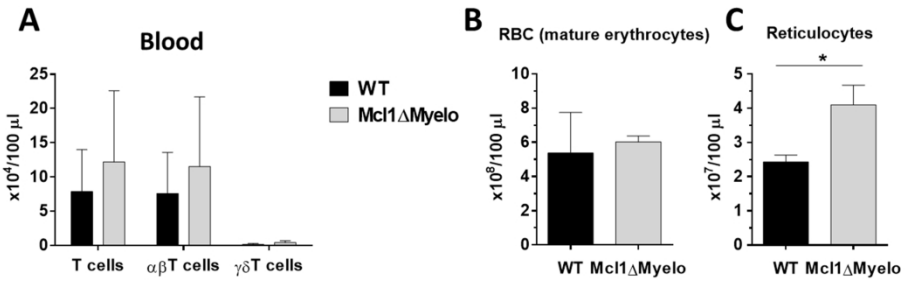


**Figure 8.** Comparison of different cellular elements within blood of WT and Mcl1ΔMyelo mice. (A) Cell numbers of main T cell subpopulations within blood of WT and Mcl1ΔMyelo mice. No significant differences were observed (n=3). (B) There is no significant difference in number of mature erythrocytes (RBC) in blood of WT and Mcl1ΔMyelo mice (n=3). (C) Blood of Mcl1ΔMyelo mice has higher number of reticulocytes compared to WT (n=3). Significance indicators: * $p<0.05$.

297x140mm (300 x 300 DPI)

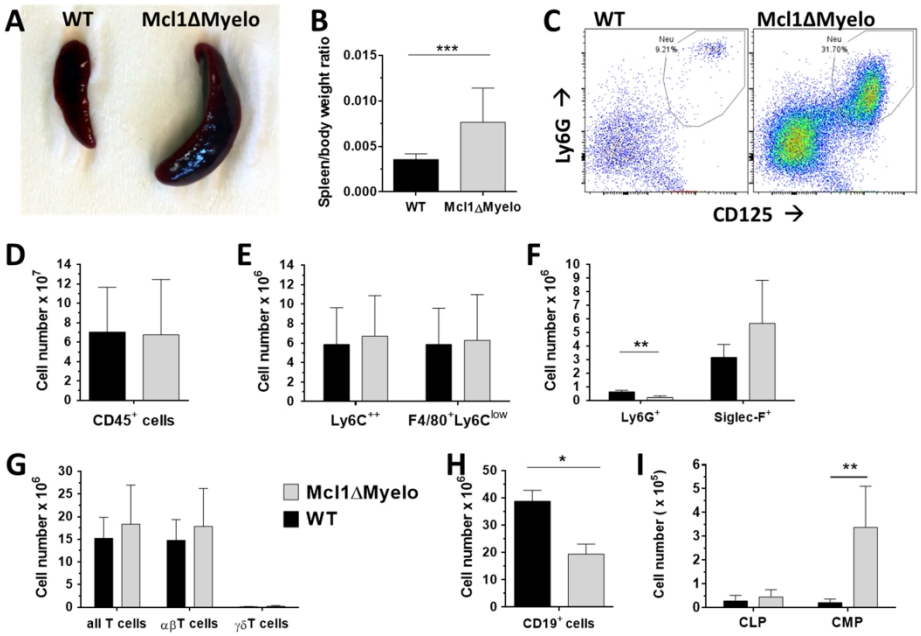


**Figure 9.** Differences in the spleen and spleen cells between WT and Mcl1ΔMyelo mice. (A) Splenomegaly was observed on multiple occasions within Mcl1ΔMyelo animals. (B) Statistical comparison of spleen/body weight ratio between WT and Mcl1ΔMyelo animals (n=20). (C) Flow cytometric measurements of living $CD45^+$ $CD11b^+$ cells. Ly6G and CD125 staining help to identify conventional $Ly6G^{++}$ neutrophils in WT animals, and atypical/immature $Ly6G^{low}$ neutrophils in spleen of Mcl1ΔMyelo mice. (D) There are no significant difference in numbers of the living $CD45^+$ leukocytes. (n=3). (E) There are no significant differences in the numbers of monocytoid $Ly6C^+$ cells or $F4/80^+$ $Ly6C^{low}$ macrophages (n=3). (F) There is significantly lower number of conventional $Ly6G^+$ neutrophils in the spleen of Mcl1ΔMyelo mice. There are no significant differences in the numbers of eosinophils (n=3). (G) There are no differences in the numbers of the indicated T cell populations (n=4). (H) There is a significant difference in number of $CD19^+$ B cells (n=4). (I) There is a significant difference in the number of common myeloid precursor cells (CMP) in the spleen, but no significant difference in the number of common lymphoid precursor cells (CLP) (n=5). Significance indicators: * $p<0.05$; ** $p<0.01$.

297x209mm (300 x 300 DPI)